

# Climate Modelling and change



Adrian Tompkins, ICTP, Trieste, Italy

Email: [tompkins@ictp.it](mailto:tompkins@ictp.it)

Version release date: July 15, 2024 These notes have benefitted from

- Brian Rose's course on climate modelling (with beautiful Jupyter notebook examples) (University of Albany)
- Thomas Stocker's excellent climate change course (University of Bern)
- Dennis Hartmann's classic, Global Physical Climatology (reference for course, chapters 9-13)
- Mcguffie and Henderson-sellers, The climate modelling primer



# Contents

<b>1</b>	<b>Modelling the atmosphere: The small stuff counts</b>	<b>5</b>
1.1	Sub-gridscale processes in the atmosphere	5
1.1.1	Parametrization concept	5
1.1.2	Turbulence processes	7
1.1.2.1	constant $K$ diffusion turbulence parametrization	7
1.1.2.2	Turbulent Kinetic Energy equation	8
1.1.2.3	higher order schemes	9
1.1.3	Convection	9
1.1.3.1	adjustment schemes	9
1.1.3.2	mass flux schemes	10
1.1.3.3	Episodic mixing models	18
1.1.3.4	Super-parameterization	18
1.1.4	Cloud microphysics	19
1.1.4.1	autoconversion to raindrops	20
1.1.4.2	rainfall evaporation	21
1.1.5	Cloud Cover	21
1.1.5.1	relative humidity schemes	23
1.1.5.2	statistical schemes	25
1.1.5.3	Defining the PDF	27
1.1.5.4	Setting the PDF moments	29
1.1.6	Diagnostic versus Prognostic schemes	30
1.1.7	A prognostic statistical scheme	31
1.1.7.1	Tiedtke scheme	34
1.1.8	Cloud overlap	35
	<b>Index</b>	<b>38</b>



# Chapter 1

## Modelling the atmosphere: The small stuff counts

### 1.1 Sub-grid-scale processes in the atmosphere

The use of a finite grid mesh implies that there are some processes that will occur on smaller scales  
Some examples (see schematic Fig. 1.1) are

- subgrid-scale motions such as local turbulence and *non-local* convection
- clouds
- radiative transfer processes
- surface exchange

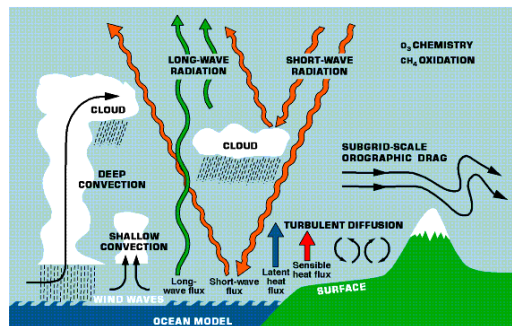


Figure 1.1: Schematic of a processes that occur on small scales and generally require parametrization in regional or global models (source: ECMWF)

Some of these processes will be discussed in part 2 and 3 of this course.

The problem is that these small-scale processes make a significant contribution to the dynamical and thermodynamic budgets.

For example, ignoring all scales of motions below the grid-scale would neglect the role of convection entirely, (and lead to grid-scale storms!) Essentially, by truncating all scales of motion at the model grid-scale, the action of small scale processes is *aliased* on the grid-scale, which would lead to significant model truncation errors.

These processes must therefore be represented by a *sub-model* called a *parametrization*, since the process is not explicitly resolved.

#### 1.1.1 Parametrization concept

To illustrate the *parametrization concept*, let us consider the barotropic vorticity equation (Eqn. 1.1).

Earliest weather forecasts integrated the Barotropic vorticity equation.

$$\frac{\partial \xi}{\partial t} + \nabla \cdot (\underline{v} \xi) + \beta \underline{v} = 0, \quad (1.1)$$

where  $\xi$  is the relative vorticity and  $\underline{v}$  the horizontal velocity vector and  $\beta$  is the poleward gradient of the Coriolis parameter. There is only one prognostic equation modelled, since the wind can be specified as a diagnostic function of the vorticity field.

We do this as it is a single simple equation to illustrate the concept, however the following analysis could be performed for the full equations of motion (Eqn. ??) if the model is based on these.

### Reynolds Averaging

We use the concept of 'Reynolds averaging'. A continuous variable  $\xi$  is defined as:

$$\xi = \bar{\xi} + \xi' \quad (1.2)$$

where  $\bar{\xi}$  is the mean of  $\xi$  in our discretised gridbox for a given model timestep, and  $\xi'$  is the *local* deviation from the average (Fig. 1.2).

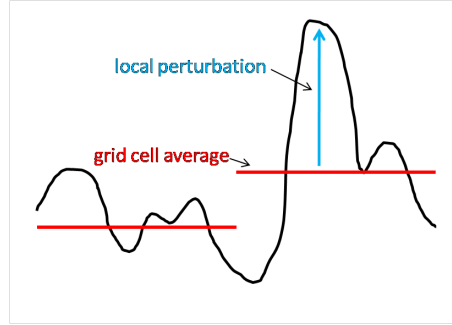


Figure 1.2: Schematic of a Reynolds averaging

Similarly  $\underline{v} = \bar{\underline{v}} + \underline{v}'$ .

Substituting into the vorticity equation we get

$$\frac{\partial \bar{\xi}}{\partial t} + \frac{\partial \xi'}{\partial t} + \nabla \cdot (\bar{\underline{v}} \bar{\xi}) + \nabla \cdot (\bar{\underline{v}} \xi') + \nabla \cdot (\underline{v}' \bar{\xi}) + \nabla \cdot (\underline{v}' \xi') + \beta \bar{\underline{v}} + \beta \underline{v}' = 0 \quad (1.3)$$

We now average this equation over the gridbox ( $\bar{\quad}$ ) and timestep, and thus applying the Reynolds averaging assumptions that

- $\bar{A}' = 0$
- $\overline{\bar{A}A'} = 0$
- $\overline{\bar{A}} = \bar{A}$

the barotropic vorticity equation reduces to

$$\frac{\partial \bar{\xi}}{\partial t} + \nabla \cdot (\bar{\underline{v}} \bar{\xi}) + \nabla \cdot (\overline{\underline{v}' \xi'}) + \beta \bar{\underline{v}} = 0 \quad (1.4)$$

We note that the equation for  $\bar{\xi}$  looks identical to that of  $\xi$ , except for the addition term  $\nabla \cdot (\overline{\underline{v}' \xi'})$ . *This term  $\nabla \cdot (\overline{\underline{v}' \xi'})$  represents the unresolved subgrid-scale processes.* This term may not be neglected, but as it stands is not specified in terms of the grid-resolved variables. There are two approaches we can take to specify  $\nabla \cdot (\overline{\underline{v}' \xi'})$ . We can

- Derive a new prognostic equation for its temporal evolution  $\frac{\partial \nabla \cdot (\overline{\underline{v}' \xi'})}{\partial t}$ . We will return to this.
- Define a *closure*, that is a diagnostic relationship that specifies  $\nabla \cdot (\overline{\underline{v}' \xi'})$  in terms of the grid-resolved variables

The purpose of parametrization is to give an expression for the subgrid-scale terms as functions of the resolved values.

In this example, one wants to determine a function  $H$  of the resolved variables such that  $\nabla \cdot (\overline{u'\xi'}) = H(\overline{\mathbf{v}}, \overline{\xi})$

By doing this the prognostic equation for the grid-scale average  $\overline{\xi}$  is written entirely in terms of grid-scale quantities, and therefore the equation set is said to be 'closed' (the same number of unknowns as equations). The function  $H$  is said to be a *parametrization*

We therefore attempt to construct a series of physical models  $H$  (that can be simple or very complicated) that use the large-scale grid resolved parameters ( $T, q, u, v, w$  etc) as *input* to determine all these subgrid-scale processes (e.g. the nature of turbulence, clouds, convection and so on). *This is parametrization task.*

These terminology 'parametrization' derives from the fact that the process in question is not explicitly modelled. The ultimate output of the parametrization scheme is the tendency of the the large-scale model equations due to the parameterized process. [Convection](#)



In the above we give examples of processes that were subgrid-scale and required representing in parametrization schemes. We will now briefly discuss more details concerning the representation of

- turbulence
- convection
- clouds

## 1.1.2 Turbulence processes

### 1.1.2.1 constant $K$ diffusion turbulence parametrization

We recall the  $K$  diffusion approach for representing turbulence. For simplicity we consider the the subgrid-scale flux in one direction only, the  $x$ -direction:

$$\frac{\partial}{\partial x} \overline{u'\xi'}. \quad (1.5)$$

We recall that we assumed turbulence led to down-scale mixing  $\overline{\xi}$ , i.e. that it leads to a situation where

$$\frac{\partial \overline{\xi}}{\partial x} = 0 \quad (1.6)$$

Let us assume that the flux of  $\overline{\xi}$  by subgrid motions is proportional to the *resolved-scale* gradient  $\frac{\partial \overline{\xi}}{\partial x}$ .

We can represent this is a simple *parametrization* by

$$\overline{u'\xi'} = -K \frac{\partial \overline{\xi}}{\partial x}, \quad (1.7)$$

where  $K$  is a constant, which we called the *diffusion coefficient*.

The diffusion coefficient  $K$  represents the strength of the subgrid-eddies, i.e. the magnitude of  $u'$ , we are assuming are always present and always of the same magnitude here, obviously a gross-oversimplification.

From the above

$$\frac{\partial}{\partial x} \overline{(u'\xi')} = -K \frac{\partial^2 \bar{\xi}}{\partial x^2} \quad (1.8)$$

Which can be substituted back in the full (1d) BVE to give:

$$\frac{\partial \bar{\xi}}{\partial t} + \frac{\partial}{\partial x} \overline{v\xi} - K \frac{\partial^2 \bar{\xi}}{\partial x^2} + \beta \bar{v} = 0 \quad (1.9)$$

or more generally:

$$\frac{\partial \bar{\xi}}{\partial t} + \nabla \cdot (\overline{v\xi}) - K \nabla^2 \bar{\xi} + \beta \bar{v} = 0 \quad (1.10)$$

Note that *the equation is now written entirely in terms of grid-mean variables*. *Q: How would you improve this parametrization for turbulence?*

### 1.1.2.2 Turbulent Kinetic Energy equation

To devise a better turbulence scheme than a simple analogy to molecular diffusion we must consider the source of subgrid-scale fluctuations. To do this we refer to the equation for the *turbulence kinetic energy (TKE)*  $\bar{e}$ :

$$\bar{e} = \frac{1}{2} (\overline{u'^2} + \overline{v'^2} + \overline{w'^2}) = \frac{1}{2} \sum_1^3 u_i^2 \quad (1.11)$$

The TKE equation is derived by multiplying the momentum equation by  $2u_i$  to get (ignoring horizontal terms as gradients are much stronger in the vertical). Here we simply give the result, where minor terms (pressure diffusion and molecular viscous transport) are neglected:

$$\frac{D\bar{e}}{Dt} = \underbrace{-0.5 \frac{\partial \overline{u'_j u'_j u'_i}}{\partial x_i}}_{\text{turbulent transport}} + \underbrace{-\overline{u'_i u'_j} \frac{\partial \overline{u_i}}{\partial x_j}}_{\text{shear production}} + \underbrace{\frac{g}{\theta} \overline{u_3 \theta'}}_{\text{Bouyancy}} - \underbrace{\epsilon_e}_{\text{dissipation}} \quad (1.12)$$

If we now consider turbulent flows in the atmosphere (and in general neglecting horizontal transport as vertical gradients are dominant), one way to derive an improved closure would be to define  $K$  in terms of the Richardson number, that describes the ratio of the key sources and sinks of turbulence in the *turbulence kinetic energy* equation, namely buoyancy and shear.

$$Ri = \frac{\frac{g}{\theta} \overline{w'\theta'}}{\overline{w'u' \frac{\partial \overline{u}}{\partial z}} + \overline{w'v' \frac{\partial \overline{v}}{\partial z}}} \quad (1.13)$$

The numerator term describes the buoyant production/suppression of turbulence, while the denominator represents the shear production.

- If  $R_{if}$  is large, buoyancy suppresses turbulence
- $0 < R_{if} < X$ , shear instabilities generate turbulence (in measurements  $X \approx 1$ , while  $X = 0.25$  in theory)
- $R_{if} < 0$  unstable lapse rate, and both buoyancy and shear generate turbulence.

An improvement of the constant  $K$  scheme can be made by letting the viscosity depend on the Richardson number.

We assume that the mixing should depend on the eddy size and the rate at which eddies are generated. Therefore on dimensional grounds (units of  $K$  are  $m^2 s^{-1}$ ):

$$K = l^2 S \quad (1.14)$$

where  $l$  is a typical length scale and  $S$  is the deformation rate

$$S^2 = 0.5 \sum_{ij} \left( \frac{\partial \overline{u_i}}{\partial x_j} + \frac{\partial \overline{u_j}}{\partial x_i} \right)^2 \quad (1.15)$$

We assume there is a local equilibrium between sources and sinks of TKE, and the shear and buoyancy terms are balanced by dissipation of turbulence by molecular friction  $\epsilon$ . Writing flux terms as  $\overline{u'_i u'_j} = K \partial u_i / \partial x_j$  (likewise for  $\theta$ ) in the Richardson number form (eqn 1.13), :

$$-KS^2 + K \frac{g}{\theta} \frac{\partial \bar{\theta}}{\partial z} = -\epsilon \quad (1.16)$$

On dimensional ground (exercise: check), we can set  $\epsilon = \frac{K^3}{l_0^4}$ , where  $l_0$  is a length scale typical of the most energetic eddies. Combining these, we get

$$l = l_0(1 - R_i)^{0.25} \quad (1.17)$$

where  $R_i$  refers to the *gradient* Richardson number

$$R_i = \frac{\frac{g}{\theta} \frac{\partial \bar{\theta}}{\partial z}}{S^2} \quad (1.18)$$

Thus we can use the parameterization  $K = l_0(1 - R_i)^{0.25}S$ .  $l_0$  is usually related to the size of the grid box used by the model, reduced in the presence of a boundary. However, some models replace this formula for  $l$  by empirical functions with different forms for stable and unstable regimes (refer e.g. to Monin Obukhov theory).

### 1.1.2.3 higher order schemes

The above approach, in which the grid mean values are prognosed and the second order terms such as  $\overline{w'\theta'}$ ,  $\overline{w'w'}$  are diagnosed (closed by defining them in terms of the grid mean values). Instead we could derive prognostic equations for these terms, which would result in 3!=6 new equations for the momentum correlations, plus additional equations for the buoyancy and other prognostic variables. These equations will contain third order terms e.g.  $\overline{u'w'\theta'}$ .

For example, the variance of the total water mixing ratio would be

$$\frac{D\overline{q'^2}}{Dt} = -\frac{\delta\overline{w'q'^2}}{\delta z} - 2\overline{w'q'}\frac{\delta\bar{q}}{\delta z} - \epsilon \quad (1.19)$$

here we are neglected turbulent transport in the horizontal, assuming vertical fluxes dominate.

The third order terms (e.g. here  $\overline{w'q'^2}$ ) either need to be closed (resulting in a *second order scheme*), or can in turn be predicted, resulting in 4th order terms. Generally higher order schemes are more accurate, but at the cost of carrying vastly more prognostic equations. See Krüger (1988) for a (rare) example of a third order scheme in action. Golaz et al. (2002a) introduce a kind of 2.5 order scheme. *First or 1.5 order schemes are still the most common approach employed.*

## 1.1.3 Convection

In this section we will provide an overview of the basics of convective parameterization approaches.

Convection schemes have to achieve a number of tasks:

- Remove convective instability and produce subgrid-scale convective precipitation (heating/drying) in unsaturated model gridboxes
- Produce a realistic mean tropical climate
- Be applicable to a wide range of scales (typical 10 - 200 km) and types of convection (deep, shallow, mid-level; tropical cyclones, squall lines, monsoon, polar lows, frontal/post-frontal convection)

### 1.1.3.1 adjustment schemes

- If convection motions were not permitted, the atmospheric temperature profile would adjust until it reached local radiative equilibrium throughout the column.
- This implies that everywhere, the radiative heating due to short-wave and infra-red absorption would be balanced by emitted radiation in the short-wave.

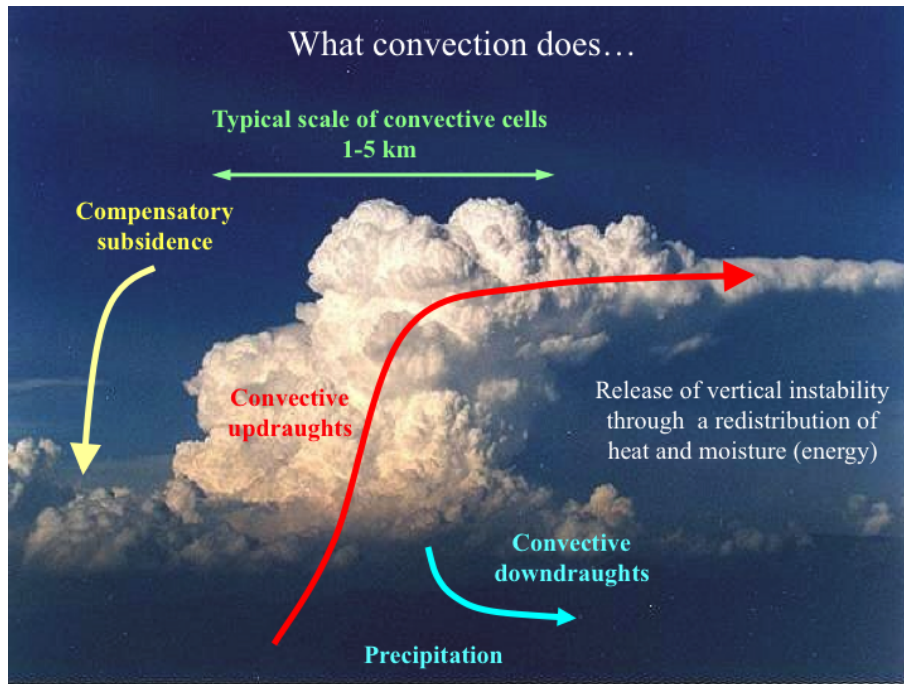


Figure 1.3: Schematic of convection role

- If one makes the calculation of radiative equilibrium, the temperature lapse rate is greater than that observed.
- This is because the lapse rate is absolutely unstable to convection - Convective overturning cools the lower atmosphere and warms the upper atmosphere

Figure 1.4 shows the temperature profile of pure radiative equilibrium, as well as a dry and moist adiabatic lapse rate.

Early convection schemes adjusted unstable lapse rates to a typical moist convective profile.

One of the most commonly used adjustment schemes was the Betts-Miller scheme [betts \(1986\)](#); [Betts and Miller \(1986\)](#). This calculated the heat and moisture fluxes implied by a readjustment to a moist adiabat, and introduced physically-based rules to determine when the adjustment occurred.)

There are issues with the adjustment approach:

- Difficult to ensure adjustment is physically consistent,
- Does not allow transport of tracers etc.

This led the move towards mass flux schemes.

### 1.1.3.2 mass flux schemes

The mass flux approach is summarized in this simplified vertical equation for potential temperature in an atmosphere in the vertical only.

$$\frac{d\theta}{dt} = Q_{ls} + \underbrace{\frac{L}{C_p}(C - E)_c + \frac{d\omega'\theta'}{dp}}_{\text{net condensation in updraughts \& convective transport}} \quad (1.20)$$

The diabatic heating term  $Q_{ls}$  refers to radiative heating as well as grid-scale (or cloud scheme) condensation/evaporation, and molecular diffusivity is neglected.

The term  $\frac{d\omega'\theta'}{dp}$  represents the transport flux by sub-grid-scale (turbulent) motions !!! **SKIP MATHS !!!!** For example, in subsidence regions (for example in the mid to upper troposphere over the Eastern Pacific), where convection may be absent,  $Q_{diab}$  is approximately zero since subsidence

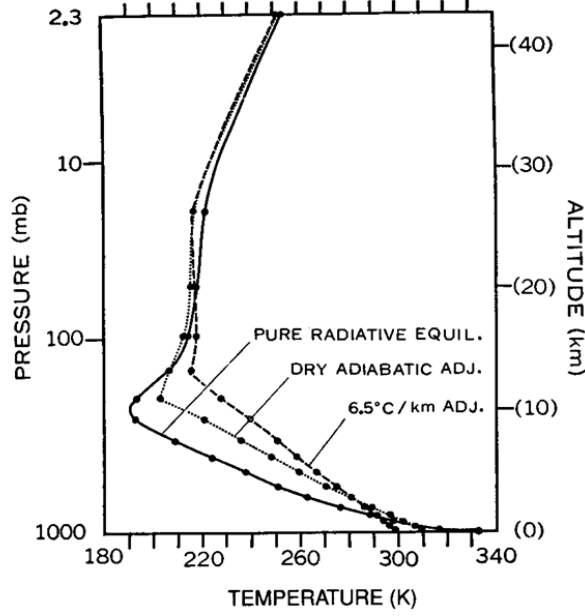


Figure 1.4: Radiative equilibrium temperature profile, dry lapse adjustment, and typical moist lapse rate used in adjustment schemes. Source (Manabe and Strickler, 1964)

heating approximately balances radiative cooling (assuming long term temperature tendencies are approximately zero). The aim of convection parametrization schemes is to define  $\frac{d\omega'\theta'}{dp}$  or more generally  $\frac{d\omega'\phi'}{dp}$ , where  $\phi$  is generic and could represent humidity, or a tracer gas etc.

To derive this we return to Reynold's averaging:

$$\overline{\omega\phi} = \overline{(\bar{\omega} + \omega')(\bar{\phi} + \phi')} \quad (1.21)$$

which gives:

$$\overline{\omega\phi} = \overline{\bar{\omega}\bar{\phi}} + \underbrace{\overline{\bar{\omega}\phi'}}_{=0} + \underbrace{\overline{\omega'\bar{\phi}}}_{=0} + \overline{\omega'\phi'}. \quad (1.22)$$

The 2nd and 3rd terms on the right are zero, and thus:

$$\overline{\omega'\phi'} = \overline{\omega\phi} - \overline{\bar{\omega}\bar{\phi}} \quad (1.23)$$

If the sum of the cumulus updraught areas= $a$  and the grid-box area is  $A$ , then the convective fraction  $\sigma$  (Fig. 1.5) is defined:

$$\sigma = \frac{a}{A} \quad (1.24)$$

Thus a quantity can be written as the weighted average of the value in convective towers  $\phi_c$ , and the value in the environment  $\phi_e$ :

$$\bar{\phi} = \sigma\phi_c + (1 - \sigma)\phi_e \quad (1.25)$$

Thus we can write

$$\overline{\omega\phi} = \sigma \underbrace{\overline{[\omega\phi]_c}}_{\text{cumulus elements}} + (1 - \sigma) \underbrace{\overline{[\omega\phi]_e}}_{\text{environment}} \quad (1.26)$$

and

$$\overline{\omega\phi} = (\sigma\bar{\omega}_c + (1 - \sigma)\bar{\omega}_e)(\sigma\bar{\phi}_c + (1 - \sigma)\bar{\phi}_e) \quad (1.27)$$

We can also apply Reynolds averaging for the cumulus elements and environment separately:

$$\overline{[\omega\phi]_c} = \bar{\omega}_c\bar{\phi}_c + \underbrace{\overline{\omega''\phi''}}_{=0} \quad (1.28)$$

The last term on the RHS is assumed zero since we neglect sub-plume *correlations*. This is known as the *top-hat approximation*. The top hat approximation is usually interpreted to imply that the

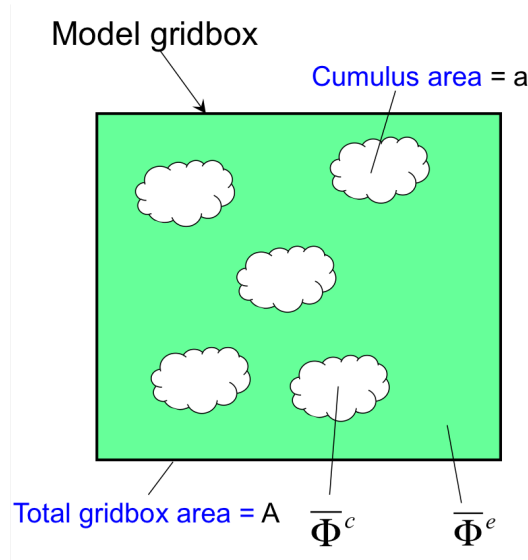


Figure 1.5: Schematic of mass flux scheme

updraught is homogeneous and sub-grid fluctuations are neglected (Fig. 1.6, although this is not strictly true. The assumption is only that the correlation between sub-plume velocity fluctuations and fluctuations in  $\phi$  is zero, implying no net transport of  $\phi$ . Inserting eqns. 1.26, 1.27 and 1.28

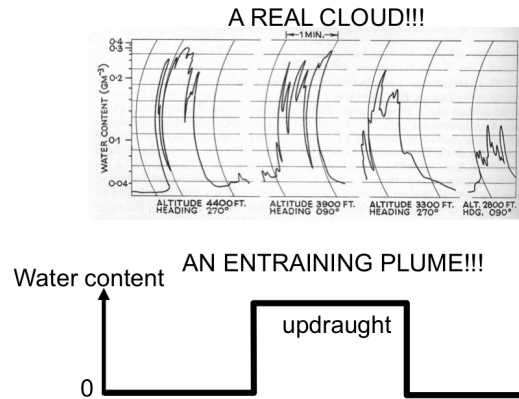


Figure 1.6: Schematic of the top hat approximation

into eqn. 1.23, one gets (*exercise*):

$$\overline{\omega' \phi'} = \sigma(1 - \sigma)(\bar{\omega}_c - \bar{\omega}_e)(\bar{\phi}_c - \bar{\phi}_e) \quad (1.29)$$

Thus the convective transport of  $\phi$  is related to the difference of the updraught speed to the environment and the perturbation of  $\phi$  in the convective core relative to the environment. In order to *close* the parametrization we would need to *specify a model to describe how both  $\sigma$  and  $\bar{\omega}_c$  change with height*. However, we can simplify this task, we can make the *small area approximation*, by assuming  $\sigma \ll 1$ , such that  $1 - \sigma \approx 1$ . We also assume that  $\omega_c \gg \omega_e$ , to allow us to neglect the latter. With these simplifications, Eqn. 1.29 reduces to

$$\overline{\omega' \phi'} = \sigma \bar{\omega}_c (\bar{\phi}_c - \bar{\phi}_e) \quad (1.30)$$

The *convective mass flux* is defined as:

$$M_c = \frac{-\sigma \bar{\omega}_c}{g} = \rho \sigma \bar{\omega}_c \quad (1.31)$$

and substituting this we get the convective mass flux equation:

$$-\overline{\omega'\phi'} = gM_c(\overline{\phi}_c - \overline{\phi}_e) \quad (1.32)$$

#### parametrization components

To predict the influence of convection on the large-scale with this approach we now need to describe:

- the convective mass flux  $M_c$
- the values of the thermodynamic (and momentum) variables inside the clouds
- the condensation/evaporation term.

This requires a *cloud model* and a *closure assumption* to determine the mass flux (at cloud base) from gridbox-averaged model variables. The early schemes using this approach solved a set of equations for an ensemble of plumes ( $M_i$ ) with a range of cloud top heights, for example [Arakawa and Schubert \(1974\)](#). This led to a very computationally intense matrix problem to solve.

AKIO ARAKAWA AND WAYNE HOWARD SCHUBERT

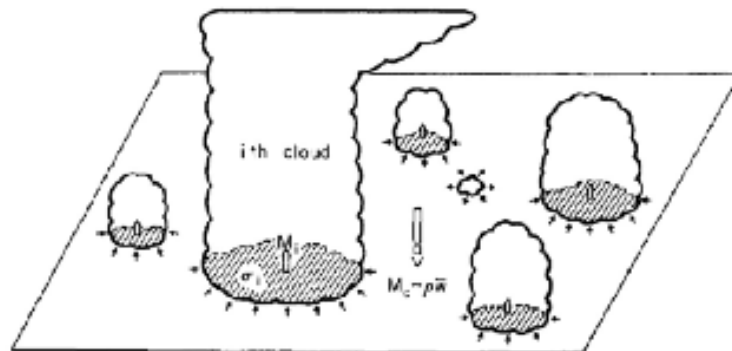


FIG. 1. A unit horizontal area at some level between cloud base and the highest cloud top. The taller clouds are shown penetrating this level and entraining environmental air. A cloud which has lost buoyancy is shown detraining cloud air into the environment.

Figure 1.7: arakawa shubert scheme

Simplifications are often made:

- Steady state plume ensemble in equilibrium
- A bulk plume model

An example is the [Tiedtke \(1989\)](#) scheme (cited approximately 2000 times).

The Tiedtke scheme introduces an equation set similar to the one described above, but without stating the assumption that  $\sigma$  is small (see equation 3 in that paper).

$$\begin{aligned} \bar{\rho}(\overline{w's'})_{cu} &= \bar{\rho} \sum_i a_{ui}(w_{ui} - \bar{w})(s_{ui} - \bar{s}) \\ &+ \bar{\rho} \sum_i a_{di}(w_{di} - \bar{w})(s_{di} - \bar{s}) \\ &+ \bar{\rho}[1 - \sum_i (a_{ui} + a_{di})](\tilde{w} - \bar{w})(\tilde{s} - \bar{s}), \end{aligned}$$

Figure 1.8: Tiedtke eqn 3

The mass flux is defined as  $M = \rho\sigma(w_c - \bar{w})$  and environmental perturbations are assumed small (small  $\sigma$  assumption).

The key equation for the updraught is simply:

$$\frac{\partial M_u}{\partial z} = E_u - D_u \quad (1.33)$$

where  $E_u$  is the fractional entrainment rate and  $D_u$  is the detrainment rate. So the model needs to define:

- The cloud base mass flux (the closure, or lower boundary condition)
- The entrainment rate
- The detrainment rate

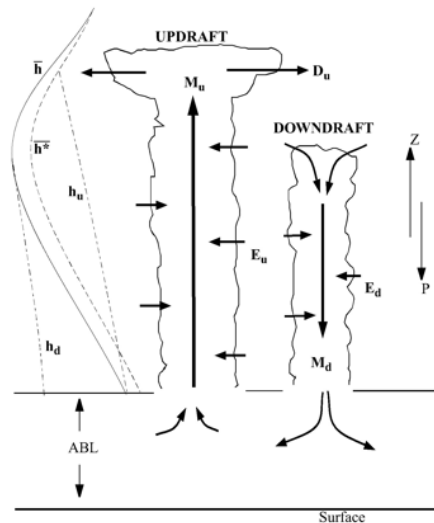


Figure 1.9: Schematic of simplified mass flux scheme such as Tiedtke (1989)

Switch to paper here:

Changes have been made to Tiedtke over time

- Entrainment is now a function of humidity - entrainment is higher in dry environments
- The closure for cloud base flux is based on the removal of CAPE over a fixed timescale.
- The detrainment profiles have been modified
- The test parcel is for a mixed boundary layer slab, not the lowest model level
- The test parcel has an excess humidity and temperature added (Q: why?)
- The numerical solver is now implicit

Step 1a: Take parcel with mean thermodynamic properties of lowest model level (Fig. 1.10)

Step 1b: Add perturbation of vertical velocity  $w$ , temperature and humidity (representing unresolved fluctuations). (Fig. 1.11)

Step 1c: Make ascent of parcel using a fixed “strong entrainment”, integrating an equation for kinetic energy (and thus  $w$ ). (Fig. 1.12)

Decision: *IF*  $w(LCL) > 0$  AND the cloud top (where  $w = 0$ ) is within 200 hPa of surface *THEN* switch on shallow convection *ELSE* test for deep convection. (Fig. 1.13)

Step 2a: Take parcel with mean thermodynamic properties of the lowest 60 hPa of troposphere, excluding the lowest model level. (Fig. 1.14)

Step 2b: Add fixed perturbations of 0.2K temperature and  $0.1\text{g kg}^{-1}$  humidity. (Fig. 1.15). What does this represent? The excess thermodynamic fluctuations are intended to represent

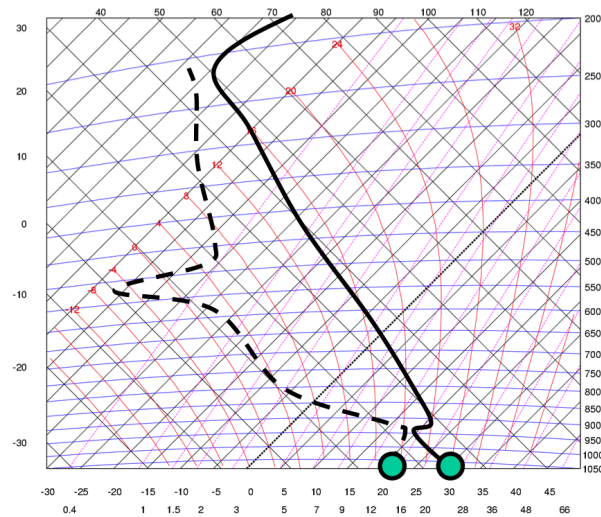


Figure 1.10: Tiedtke (CY36R1) Mass flux logic

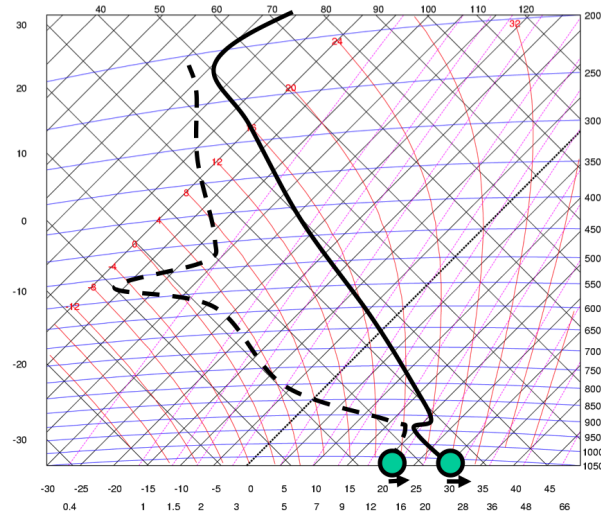


Figure 1.11: Tiedtke (CY36R1) Mass flux logic

subgrid-scale variability. But their fixed values implies that they are not related to or consistent with other assessments of sub-gridscale variability in the model (e.g. other parts of the convection scheme, radiation, clouds etc).

Starting from  $w = 1 \text{ m s}^{-1}$  do a parcel ascent, again integrating a w-equation until  $w=0$ , with low entrainment rate and partial rain-out (Fig. 1.16).

Decision: *IF* cloud top more than 200 hPa from parcel origin *THEN* deep convection activated, *ELSE* test each individual layer to 700 hPa. (Fig. 1.17)

Step 3 Mid level convection: Test for instability to mid-level convection for any level above 500m, where  $RH > 80\%$ . (Fig. 1.18) The process is highly “discrete” and “discontinuous” with many thresholds and switching processes. This makes it hard to introduce a scheme that smoothly switches off as resolution increases.

#### entrainment

#### ESCAPE

#### Entrainment

A large uncertainty remains on how to specify the entrainment of environmental air into the convective plume and the detrainment of cloudy air into the environment. Only indirect estimates are available from a limited number of field experiments.

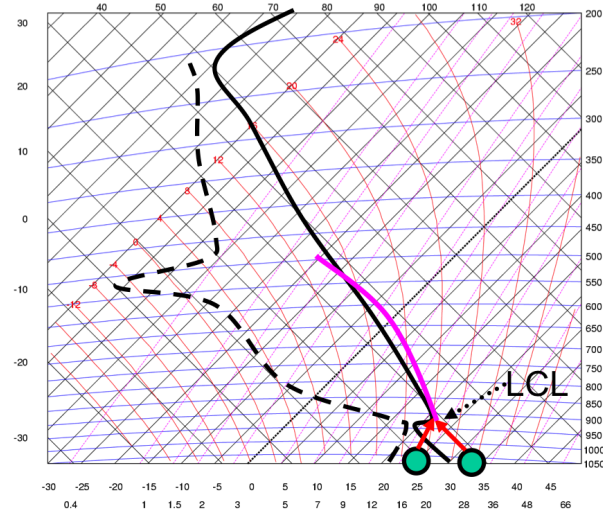


Figure 1.12: Tiedtke (CY36R1) Mass flux logic

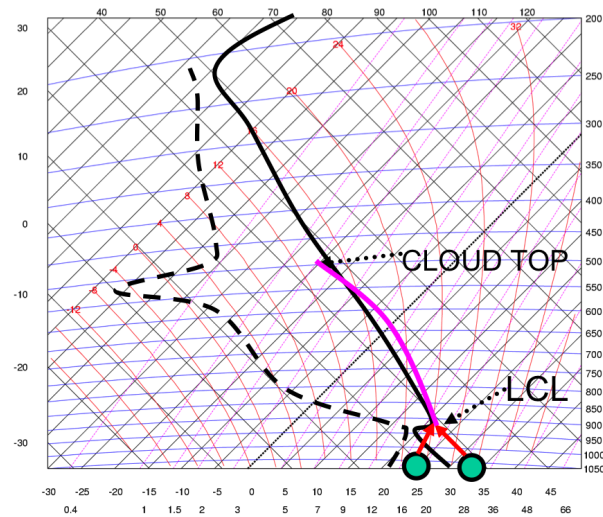


Figure 1.13: Tiedtke (CY36R1) Mass flux logic

It is commonly assumed that:

- Shallow convective clouds entrain more than deep convective clouds.
- Entrainment is maximum close to cloud base and diminishes upwards (Yanai, 1973)(Yanai et al., 1973).
- Detrainment is maximum close to cloud top (anvils).

A few examples of formulations for entrainment rates:

- $E = f(R)$  ( $R$  = cloud radius), (e.g. Simpson and Wiggert, 1969)
- $E = f(1/z)$  for shallow convection, (e.g. de Roode et al., 2000; Jakob, 2003)
- $E = \text{constant}$  : Until recently used in Tiedtke (1989) ECMWF scheme
- $E = f(RH)$  New ECMWF formulation, low RH implies high entrainment. *justification?*

microphysics SKIP SECTION

microphysics

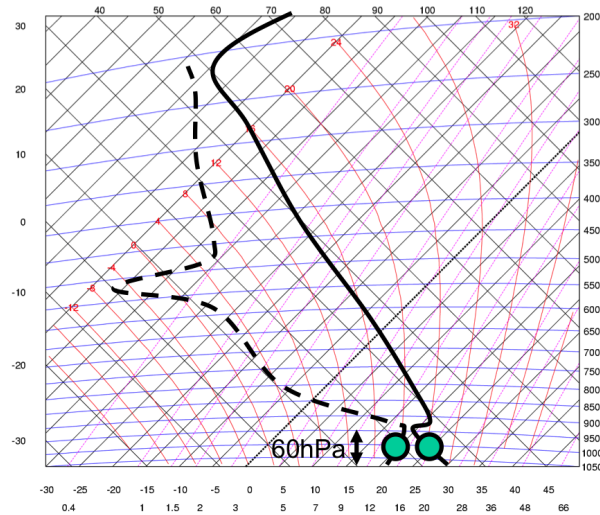


Figure 1.14: Tiedtke (CY36R1) Mass flux logic

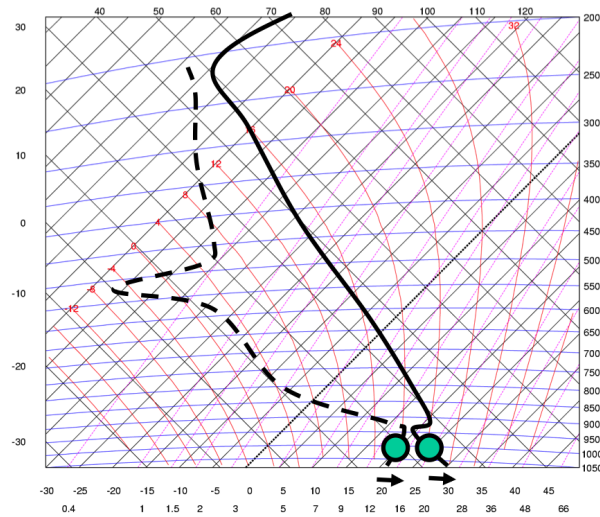


Figure 1.15: Tiedtke (CY36R1) Mass flux logic

Microphysics in updraughts is simple, with a Kessler or Sundqvist type equation integrated for the Lagrangian parcel in the final ascent.

Kessler (1969):

$$\frac{dq_l}{dt} = K(q_l - q_{crit}) \text{ if } q_l > q_{crit} \quad (1.34)$$

Where  $K$  is a rate conversion constant and  $q_l$  is the critical mass mixing ratio at which raindrop collection processes become efficient (drops are present that exceed 20 microns radius). No information about the updraught speed is used. **downdraughts**

### Downdraughts

Downdraughts are often treated very simply. The routine finds the highest level of free sinking (LFS) for which an equal saturated mixture of cloud and environmental air becomes negatively buoyant (Eqn. 1.35):

Tiedtke (1989) simply relates the “seed” downdraught mass flux to the updraught base mass flux.

$$M_{d,b} = -0.3M_{u,b} \quad (1.35)$$

**closure** Example of a closure: Convection counteracts destabilization of the atmosphere by large-scale processes and radiation - Stability measure used: CAPE

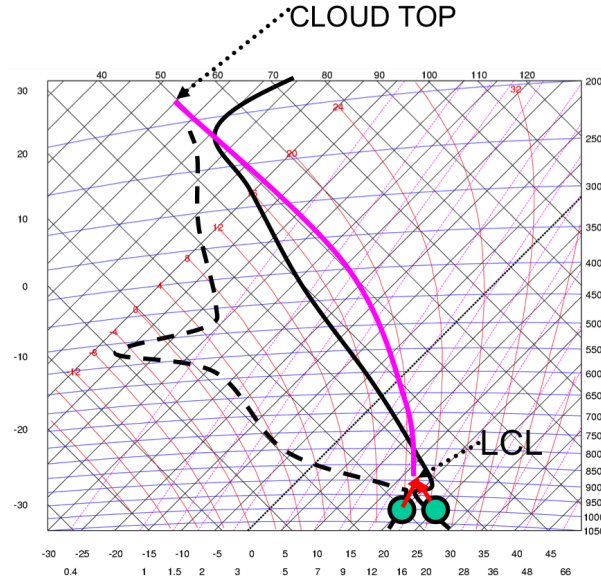


Figure 1.16: Tiedtke (CY36R1) Mass flux logic

Assume that convection reduces CAPE to 0 over a given timescale, i.e.,

$$\frac{dCAPE}{dt} \Big|_{cu} = -\frac{CAPE}{\tau} \quad (1.36)$$

### 1.1.3.3 Episodic mixing models

Emanuel (1991) followed on from Paluch (1979) and Raymond and Blyth (1986) to suggest an episodic mixing model (Fig. 1.23) in which multiple plumes were calculated, each undergoing different mixing quantities with the environment

### 1.1.3.4 Super-parameterization

Another approach is super parameterization, whereby a 2 or 3 dimensional cloud resolving model is inserted into each grid-box of the GCM (Randall et al., 2003). *Q: Advantages and disadvantages?*

This approach was first suggested and successfully implemented in a intermediate complexity GCM by ?, and has since been taken up as an option of the north American community climate model by the group of David Randall at Colorado State University as well as receiving attention by Arakawa.

The approach allows you one to omit a considerable number of parameterization assumptions due to the (crude) resolution of convective processes. For example, the overlap of clouds in the vertical is handled explicitly and does not require parameterization. The impact of vertical windshear on the tilting of updraughts and the enhancement of sub-cloud rainfall evaporation is also explicitly included, effects that are usually omitted from conventional parameterization approaches, or handled in an ad hoc way.

That said, the numerical expense of include more than a few hundred horizontal grid-points at best in the sub-grid model means that the meso-scale is still omitted, and the jury is still out as to whether global climate models using such schemes out perform standard approaches. Surprisingly, there is evidence that such models can nevertheless represent the advection of squall-line-like feature between cells of the host global model.

Conclusions:

- Parametrization introduces a sub-grid model to represent small-scale, unresolved physics
- Deep convection schemes represent the effect of non-local transport
- Early schemes were based on the adjustment approach

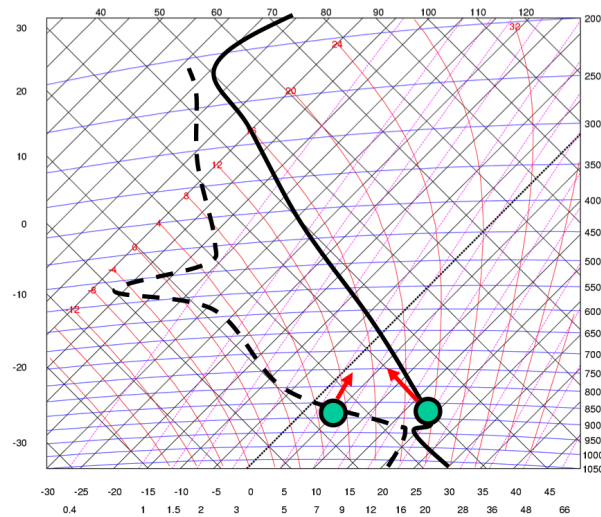


Figure 1.17: Tiedtke (CY36R1) Mass flux logic

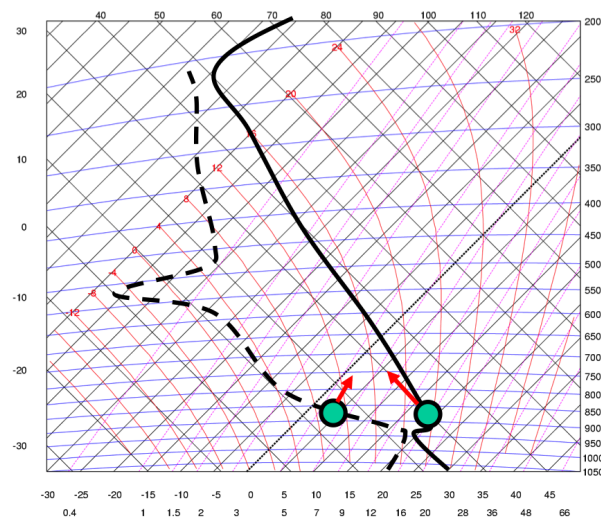


Figure 1.18: Tiedtke (CY36R1) Mass flux logic

- Mass flux are the mainstay of parametrization, even today
- Bulk assumption has weaknesses, addressed in the multi-plume approach
- move towards super-parameterization, but at the expense of computing

#### 1.1.4 Cloud microphysics

There are two key tasks regarding cloud parameterization. The representation of the cloud geometry (cloud macrophysics) and the processes that convert water between the various phases (cloud microphysics).

A typical simple microphysics parametrization is shown in Fig. 1.25. Each yellow box represents a prognostic equation for the mass mixing ratio of a bulk water quantity, while the arrowed pathways indicates processes that transfer water from one category to another.

##### Condensation/Evaporation

Since the diffusional growth of cloud droplets in supersaturated conditions is very rapid (cf. global model timestep), it can be assumed that all excess (supersaturated) water vapour immediately condenses into cloud water droplets. Likewise in subsaturated conditions, all cloud drops immediately evaporate.

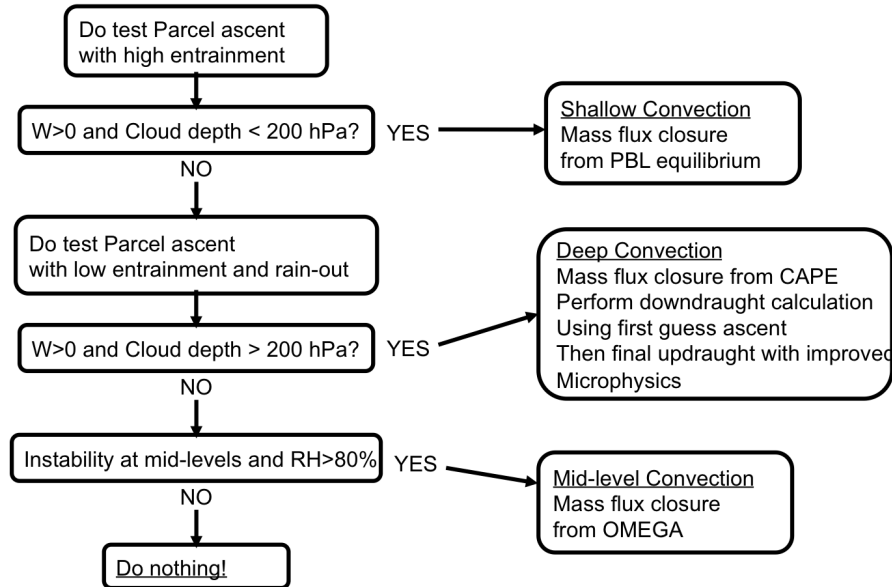


Figure 1.19: Schematic of mass flux logic chain

What information does this not provide?

Assuming fast condensation timescales implies that for warm processes, a single prognostic equation for the total water may be employed, which is divided into liquid cloud water and water vapour according to temperature:  $r_t = r_v + r_l$  where  $r_l = r_t - r_s(T, p)$ . No information concerning the cloud droplet number (related to the CCN) is provided. Either the droplet number is diagnosed (e.g. fixed, or related to aerosol from a climatology or an online aerosol scheme), or it can be prognosed from sources and sinks. The latter approach is referred to as a *double moment scheme* as two moments, the mass mixing ratio and the droplet number are predicted.

#### 1.1.4.1 autoconversion to raindrops

Autoconversion from cloud droplets to raindrops is a highly nonlinear process, and only becomes efficient when there is a wide range of cloud drop sizes. Knowledge of the droplet size distribution is usually lacking in the global model, and therefore diagnostic assumptions have to be made. This results in a wide variety of schemes

Kessler (1969):

$$\frac{dq_l}{dt} = A(q_l - q_{crit}) \text{ if } q_l > q_{crit} \quad (1.37)$$

Sundqvist et al. (1989):

$$\frac{dq_l}{dt} = Aq_l(1 - e^{-(\frac{q_l}{q_{crit}})^2}) \quad (1.38)$$

Beheng (1994):

$$\frac{dq_l}{dt} = Aq_l^M \quad (1.39)$$

Here,  $A$  is simply a constant, and  $q_{crit}$  is the critical mass mixing ratio at which the autoconversion process becomes efficient. In order for the creation of raindrops to become efficient a wide range of cloud droplet sizes is required to get a wide range of fallspeeds, with some of the largest drops requiring a radius exceeding 20 microns. Therefore, if an assumption is made concerning the distribution of dropsizes, and also the droplet concentration number (related to the number of cloud condensation nuclei, CCN you will recall), then the critical radius for the maximum dropsizes can be converted into a critical mean mass mixing ratio. See the paper of Liu et al. (2006) for an intercomparison of the many autoconversion approaches, and a suggested generalization of these.

It is possible to alter the constant  $A$  to account for collision and accretion processes:

$$A = A_0 q_c q_r^{7/8} \quad (1.40)$$

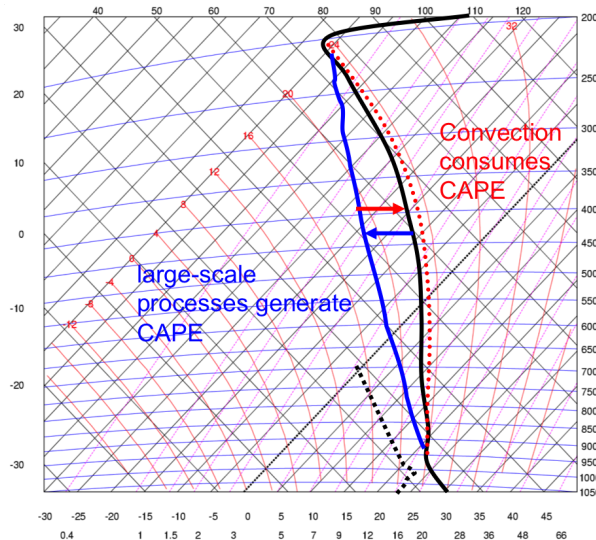


Figure 1.20: Schematic of mass flux logic chain

The form and the constants vary from scheme to scheme.

#### 1.1.4.2 rainfall evaporation

Rainfall evaporation will depend on the relative humidity  $RH$  of the air through which rain is falling, and the magnitude of the rainfall flux, related to the rain mass mixing ratio  $q_r$ .

$$\frac{dq_r}{dt} = X_1(1 - RH)q_r^{X_2} \quad (1.41)$$

$X_1$  and  $X_2$  are not true constants as they contain density terms. The evaporation rate is in reality controlled by the rate at which heat can diffuse to balance the latent heat of vaporisation.

Most current models have microphysics schemes on the order of complexity of that shown in Fig. 1.26, with additional prognostic equations for ice. We will not focus on the details of the microphysics here, refer to [Lohmann and Roeckner \(1996\)](#) for an example of a scheme. Instead let us consider the macrophysics of clouds

#### 1.1.5 Cloud Cover

When considering the approach to model clouds in general circulation models (GCMs), there are a number of zero order *cloud macrophysical* issues that require attention, in addition to the representation of the complex warm phase and ice phase microphysics processes that govern the growth and evolution of cloud and precipitation particles.

Unlike cloud resolving models (CRMs) or large-eddy models (LEMs), which, having grid resolutions finer than  $O(1\text{km})$ , aim to resolve the motions relevant for the clouds under consideration, GCMs must additionally consider macroscopic geometrical effects. Claiming to resolve cloud scale motions allows CRMs and LEMs to make the assumption that each grid scale is completely cloudy if condensate is present. This approach is clearly not adequate for GCM size grid scale of  $O(100\text{km})$  for which clouds are a subgrid-scale phenomenon, (although some schemes such as [Ose, 1993](#); [Fowler et al., 1996](#), have indeed adopted this approach).

GCMs must consider cloud geometrical effects. To reduce the fractal cloud to a tractable low dimensional object, GCMs usually reduce the problem to the specification of the:

- horizontal fractional coverage of the gridbox by cloud,
- vertical fractional coverage of the gridbox by cloud,
- sub-cloud variability of cloud variables in both the horizontal and vertical, and the
- overlap of the clouds in the vertical column

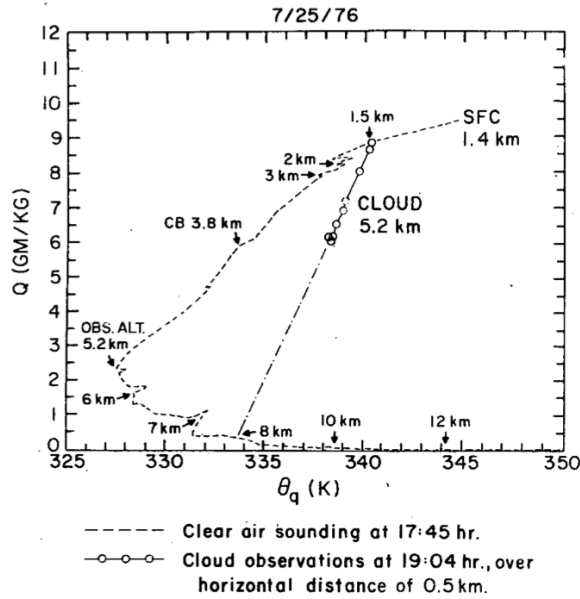


Figure 1.21: Mixing diagram from Paluch (1979)

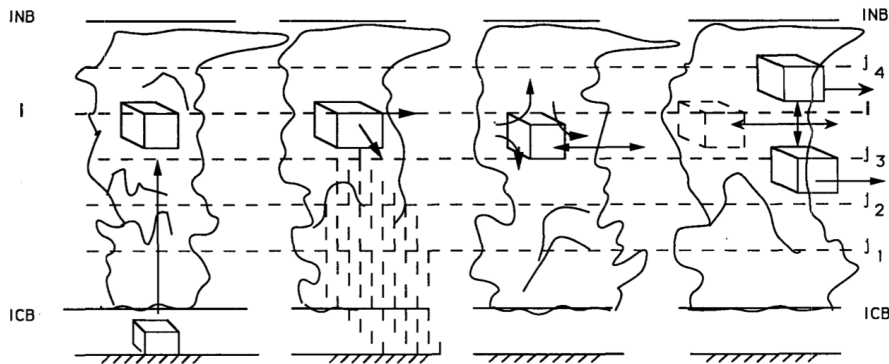


Figure 1.22: Schematic of the episodic mixing model approach, see Emanuel (1991) for details.

The above list is far from exhaustive, and implicitly neglects interactions between adjacent GCM columns (for example, how cloud affects solar fluxes in adjacent columns at low sun angles), probably a safe assumption for grid-scales exceeding 10km or so (Giuseppe and Tompkins, 2003).

In fact, most GCMs further simplify the above list (i) by assuming clouds fill GCM grid boxes in the vertical and (ii) by neglecting many of the consequences of sub-cloud fluctuations of cloud properties. Both of these are considerable simplifications. Although vertical GCM grids are much finer than the horizontal resolution, the same is of course also true of cloud processes. Using  $O(50)$  levels in the vertical implies that some cloud systems or microphysical related processes are barely if at all resolved, such as tropical thin cirrus (Dessler and Yang, 2003), or the precipitation melting layer (Kitchen et al., 1994), which can have important implications (Tompkins and Emanuel, 2000). Likewise, many authors have highlighted the biases that can be introduced when sub-cloud fluctuations are neglected, due to the strong nonlinearity of cloud and radiative processes (Cahalan et al., 1994; Barker et al., 1999; Pincus and Klein, 2000; Pomroy and Illingworth, 2000; Fu et al., 2000; Rotstajn, 2000; Larson et al., 2001a).

Nevertheless, the zero order primary task of cloud schemes, in addition to representing the microphysics of clouds, is to predict the horizontal cloud coverage. It is clear that a utopian perfect microphysical model will render poor results if combined with an inaccurate predictor of cloud cover, due to the incorrect estimate of in-cloud liquid water. This introductory course presents the general approaches used to date in GCMs for this task.

The first thing to realize is that fractional cloud cover can *only* occur if there is horizontal

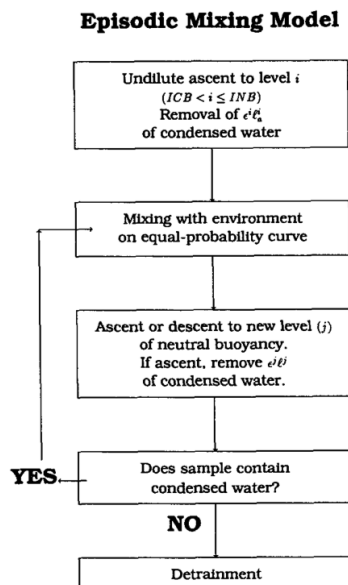


Figure 1.23: Decision tree of the episodic mixing model approach, see Emanuel (1991) for details.

subgrid-scale variability in humidity and/or temperature (controlling the saturation mixing ratio,  $q_s$ ). If temperature and humidity are homogeneous, then either the whole grid box is subsaturated and clear, or supersaturated and cloudy<sup>1</sup>.

This is illustrated schematically in Fig. 1.27. Fluctuations in temperature and humidity may cause the humidity to exceed the saturated value on the subgrid scale. If it is assumed that all this excess humidity is immediately converted to cloud water (and likewise that any cloud drops evaporate instantly in subsaturated conditions), then it is clear that the grid-mean relative humidity ( $\overline{RH}$ , where the overline represents the gridbox average) must be less than unity if the cloud cover is also less than unity, since within the cloudy parts of the gridbox  $RH = 1$  and in the clear sky  $RH < 1$ . Generally speaking, since clouds are unlikely when the atmosphere is dry, and since  $RH$  is identically 1 when  $C = 1$ , there is likely to be positive correlation between  $RH$  and  $C$ .

The main point to emphasize is that, *all* cloud schemes that are able to diagnose non-zero cloud cover for  $\overline{RH} < 1$  (i.e. any scheme other than an “all-or-nothing” scheme) must make an assumption concerning the fluctuations of humidity and/or temperature on the subgrid-scale, as in Fig. 1.27. Either (i) they will *explicitly* give the nature of these fluctuations, most usually by specifying the probability density function (PDF) for the total water at each gridcell, or (ii) they will *implicitly* assume knowledge about the time-mean statistics of the fluctuations (i.e. the actual PDF at each grid point is maybe not known).

It is important to recall, when trying to categorize the seemingly diverse approaches to cloud cover parametrization, that *this central fact ties all approaches together*.

### 1.1.5.1 relative humidity schemes

*Relative humidity schemes* are called such because they specify a diagnostic relationship between the cloud cover and the relative humidity.

In the last section we saw that subgrid-scale fluctuations allow cloud to form when  $\overline{RH} < 1$ .  $RH$  schemes formalize this by setting a critical  $RH$  (denoted  $RH_{crit}$ ) at which cloud is assumed to form, and then increase  $C$  according to a monotonically increasing function of  $RH$ , with  $C=1$  identically when  $RH=1$ .

One commonly used function was given by Sundqvist et al. (1989):

$$C = 1 - \sqrt{\frac{1 - RH}{1 - RH_{crit}}} \quad (1.42)$$

<sup>1</sup>For simplicity, throughout this text we ignore the subtle complication of the ice phase, where supersaturations are common (Heymsfield et al., 1998; Gierens et al., 2000; Spichtinger et al., 2003)

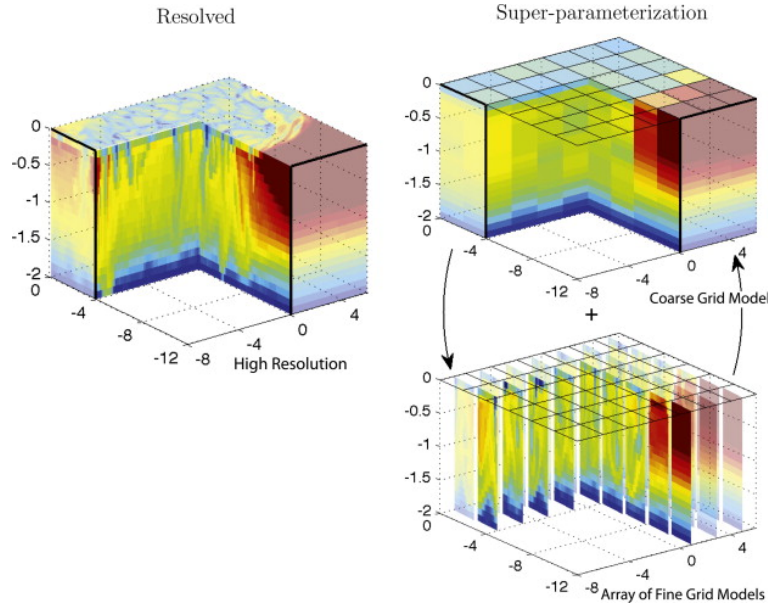


Figure 1.24: Schematic of super-parameterization approach

Thus it is apparent that  $RH_{crit}$  defines the *magnitude of the fluctuations of humidity (the humidity variance)*. If  $RH_{crit}$  is small, then the subgrid humidity fluctuations must be large, since cloud can form in dry conditions.

It is clear that one of the drawbacks of this type of scheme is that the link between cloud cover and local dynamical conditions is vague. Convection will indeed produce cloud if its local moistening effect is sufficient to increase  $RH$  past the critical threshold, but it is apparent that a grid cell with 80%  $RH$  undergoing deep convection is likely to have different cloud characteristics than a gridcell with 80%  $RH$  in a frontal stratus cloud.  $RH$  schemes simply state that, averaged across all conditions across the globe, a gridcell with X%  $RH$  will have Y% cloud cover.

This lack of differentiation between different local conditions lead some authors to augment their  $RH$  schemes using additional predictors.

The ECHAM4 climate model [Roeckner et al. \(1996\)](#) augments the cloud cover in the presence of a strong temperature inversion to improve the representation of stratocumulus.

The [Slingo \(1980, 1987\)](#) scheme predicts the mid-level cloud cover ( $C_{mid}$ ) as

$$C_{mid}^* = \left( \frac{RH - RH_{crit}}{1 - RH_{crit}} \right)^2, \quad (1.43)$$

but Slingo modifies this according to an additional predictor, the vertical velocity at 500 hPa ( $\omega_{500}$ ), thus

$$C_{mid} = C_{mid}^* \frac{\omega_{500}}{\omega_{crit}}, \quad (1.44)$$

if  $0 > \omega_{500} > \omega_{crit}$  while the cloud cover is set to zero if subsidence is occurring ( $\omega_{500} > 0$ ).

Likewise [Xu and Randall \(1996\)](#) used a cloud resolving model (CRM) to derive an empirical relationship for cloud cover based on the two predictors of  $RH$  and cloud water content:

$$C = RH^p \left[ 1 - \exp \left( \frac{-\alpha_0 \bar{q}_l}{(q_s - q_v)^\gamma} \right) \right], \quad (1.45)$$

where  $\gamma$ ,  $\alpha_0$  and  $p$  are 'tunable' constants of the scheme, with values chosen using the CRM data. *Q: what is the weakness of such an approach?* One weakness of such a scheme is, of course, this dependence on the reliability of the CRM's parametrizations, in particular the microphysics scheme. Additionally, it is unlikely that the limited set of (convective) cases used as the training dataset used would encompass the full range of situations that can naturally arise, such as cloud in frontal systems for example.

While these latter schemes use additional predictors for cloud cover, we shall still refer to them as "relative humidity" schemes, since the common and central predictor in all cases is  $RH$ . It is

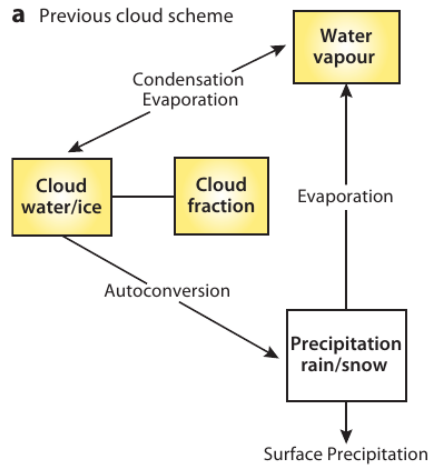


Figure 1.25: Schematic of a very simple microphysics scheme previously at use in ECMWF. (source: ECMWF Tech memo 649)

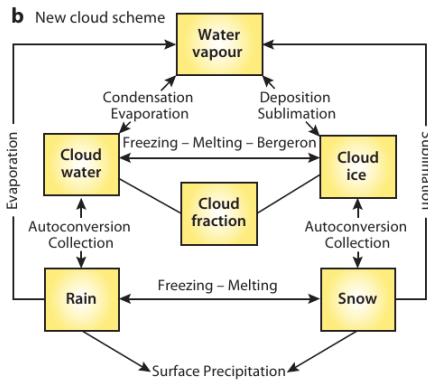


Figure 1.26: Schematic of the present bulk microphysics scheme in use at ECMWF (source: ECMWF Tech memo 649)

doubtful if any of the schemes could be reasonably simplified by replacing the  $RH$  dependence with a fixed value.

### 1.1.5.2 statistical schemes

Instead of describing the spatial and temporal mean statistics of the humidity fluctuations such as the  $RH$  schemes, another group of schemes take a different approach, *by specifying the underlying distribution of humidity (and/or temperature) variability at each grid box*. These are referred to as *statistical schemes*. This is shown schematically in Fig. 1.28.

If the PDF form for total water  $q_t$  is known, then the cloud cover is simply the integral over the part of the PDF for which  $q_t$  exceeds  $q_s$ :

$$C = \int_{q_s}^{\infty} G(q_t) dq_t, \quad (1.46)$$

Likewise, the cloud condensate is given by

$$\bar{q}_c = \int_{q_s}^{\infty} (q_t - q_s) G(q_t) dq_t. \quad (1.47)$$

As always we are assuming that all supersaturation is immediately condensed as cloud. Here we are also ignoring temperature fluctuations for simplicity, but these can be included.

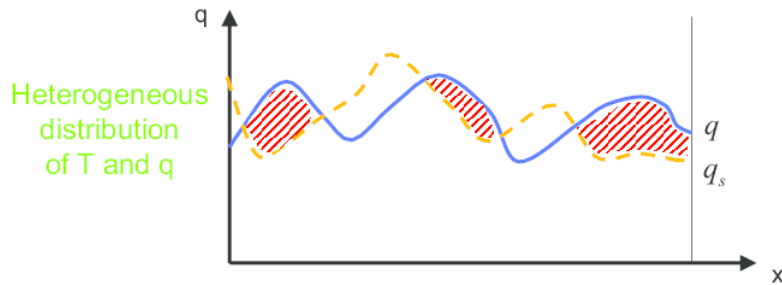


Figure 1.27: Schematic showing that partial cloud cover in a gridbox is only possible if temperature or humidity fluctuations exist. The blue line shows humidity and the yellow line saturation mixing ratio across an arbitrary line representing a gridbox. If all supersaturation condenses as cloud then the shaded regions will be cloudy.

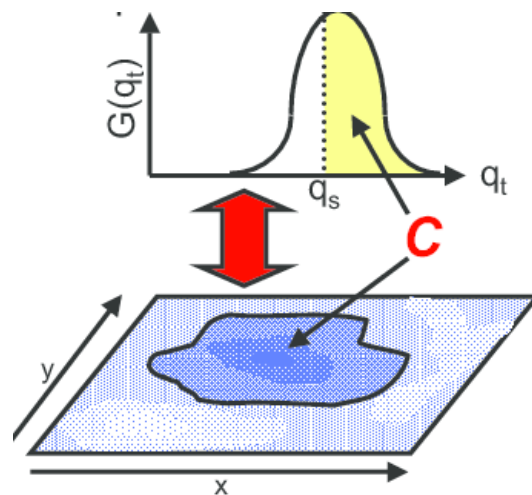


Figure 1.28: Schematic showing the statistical scheme approach. Upper panel shows an idealized PDF of total water ( $q_t$ ). The vertical line represents the saturation mixing ratio  $q_t = q_s$ , thus all the points under the PDF to the right of this line are cloudy. The integral of this area translates to the cloudy portion of the gridbox, marked on the lower part of the figure, with darker shading schematically representing high total water values.

Table 1.1: PDF forms used in statistical cloud schemes. In the summary column, the key is: U=unimodal, B=Bimodal, S=Symmetric, Sk=Skewed.

PDF Shape	Summary	Reference
Double Delta	U,S	Ose (1993); ?
Uniform	U,S	LeTreut and Li (1991)
Triangular	U,S	Smith (1990); Rotstayn (1997); Nishizawa (2000)
Polynomial	U,S	Lohmann et al. (1999)
Gaussian	U,S	?Ricard and Royer (1993); Bechtold et al. (1995)
Beta	U,Sk	Tompkins (2002)
Log-normal	U,Sk	Bony and Emanuel (2001)
Exponential	U,Sk	?Ricard and Royer (1993); Bechtold et al. (1995)
Double Gaussian/Normal	B,Sk	Lewellen and Yoh (1993); Golaz et al. (2002b)

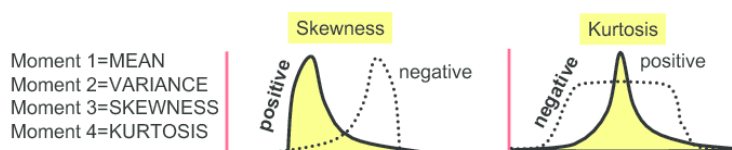


Figure 1.29: Schematic illustrating the 3rd and 4th moments; skewness and kurtosis

The main tasks of the statistic scheme is therefore to give a suitable form for the PDF of total water fluctuations, and to derive its defining moments.

Schemes can be either diagnostic or prognostic in nature. Prognostic means that a separate equation is introduced with memory of the PDF moments, that evolve in time. Diagnostic implies that the PDF characteristics are instead defined in terms of other available variables (e.g. RH, cloud water content). Examples of prognostic PDF schemes are given in Golaz et al. (2002a) (fully self-consistent but no ice processes) and Tompkins (2002) (simplified approach, but includes ice microphysics).

The main tasks of the statistic scheme is therefore to give a suitable form for the PDF of total water fluctuations, and to derive its defining moments.

### 1.1.5.3 Defining the PDF

Various distributions have been used, many of which are symmetrical. Smith (1990) uses a symmetric triangular PDF, diagnosing the variance based on a critical RH function at which cloud is determined to form, later modified by Cusack et al. (1999). This PDF has been subsequently adopted by Rotstayn (1997) and Nishizawa (2000). LeTreut and Li (1991) use a uniform distribution, setting the distribution's variance to an arbitrarily defined constant. A Gaussian-like symmetrical polynomial function was used by Lohmann et al. (1999) with variance determined from the subgrid-scale turbulence scheme following Ricard and Royer (1993), who investigated Gaussian, exponential and skewed PDF forms. Bechtold et al. (1992) based their scheme on the Gaussian distribution, which was modified in Bechtold et al. (1995) to a PDF linearly interpolated between Gaussian and exponential distributions. Bony and Emanuel (2001) have introduced a scheme that uses a generalized Log-Normal distribution. Lewellen and Yoh (1993) detail a parameterization that uses a Bi-normal distribution that can be skewed as well as symmetrical and is bimodal, although a number of simplifying assumptions were necessary in order to make the scheme tractable. Likewise Golaz et al. (2002b) also give a bimodal scheme. These forms are summarized in table 1.1 and drawn *schematically* in Fig. 1.30.

Examples of PDFs measured in the literature are shown in Fig. 1.31. Although it is difficult to theoretically derive a PDF form, since the  $q_t$  distribution is the result of a large number of interacting processes, therefore forcing the use of empirical methods, it is possible to use physically-based arguments to justify certain functional forms. For example, in the absence of other processes, large-scale dynamical mixing would tend to reduce both the variance and the asymmetry the distribution. Therefore, the Gamma and Lognormal distributions would be difficult to use since

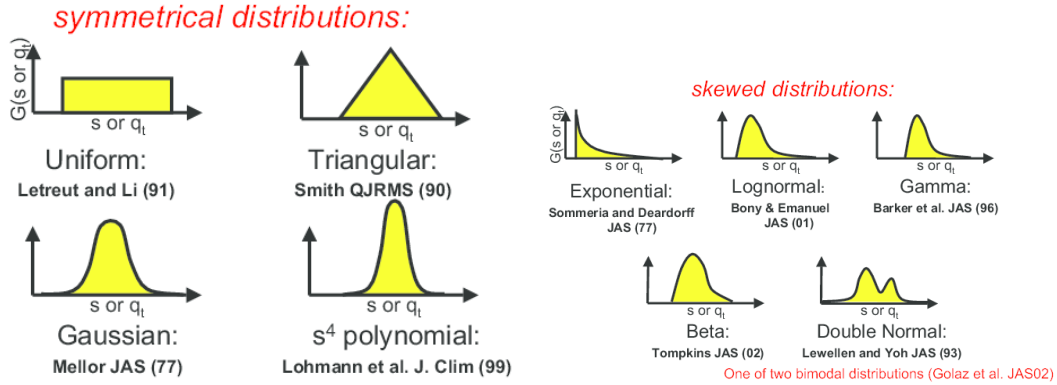


Figure 1.30: Schematic of PDF forms for  $G(q_t)$  used to date, divided into symmetrical and skewed categories. The papers referred to are: Letreut and Li (1991); Smith (1990); Mellor (1977); Lohmann et al. (1999); Sommeria and Deardorff (1977); Bony and Emanuel (2001); Barker et al. (1996); Tompkins (2002); Lewellen and Yoh (1993). Note that Barker et al. (1996) is not describing a cloud scheme, but a corrective mechanism for radiative biases that assumed this distribution for in-cloud water fluctuations.

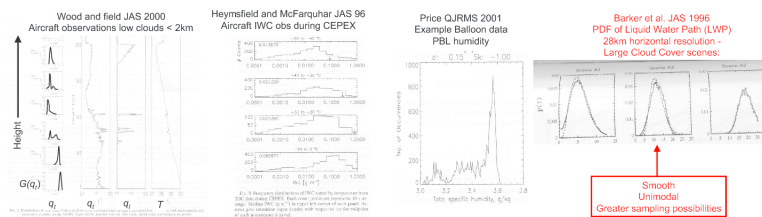


Figure 1.31: Reproduction of LWP, ice water content and total water PDFs from various observational studies. The papers referred to are: Wood and Field (2000); Heymsfield and McFarquhar (1996); Price (2001); ?.

they are always positively skewed, and only tend to a symmetrical distributions as one of their defining parameters approaches infinity. [Bony and Emanuel \(2001\)](#) attempt to circumnavigate this by switching between Lognormal and Gaussian functions at a threshold skewness value.

Another problem that distributions such as the Lognormal, Gamma, Gaussian and Exponential suffer from is that they are all unbounded functions. Thus, if these functional forms are used, the maximum cloud condensate mixing ratio approaches infinity, and part of the grid cell is always covered by cloud. Precautionary measures, such as the use of a truncated function, can be taken, but this increases the number of parameters required to describe the distribution, and again introduces undesirable discreteness. Moreover, functions such as the Gaussian function or the polynomial used by [Lohmann et al. \(1999\)](#) are also negatively unbounded, implying that part of the gridcell has negative water mass. The choice of function must also involve a fair degree of pragmatism, since in addition to providing a good fit to the available data, it must also be sufficiently simple and of few enough degrees of freedom to be of use in a parameterization scheme. For example, [Larson et al. \(2001b\)](#) were able to provide good fits to their aircraft data using a 5-parameter double Gaussian function, but it is unclear how these parameters would be determined in a GCM cloud scheme. The Beta distribution used by [Tompkins \(2002\)](#) is bounded and can provide both symmetrical and skewed distributions, but has the disadvantage of an upper limit on the skewness when the distribution is restricted to a sensible bell-shaped regime, and that the form is not mathematically as simple as alternative unimodal distributions.

Considering the question of whether a unimodal distribution is necessary, we refer to a number of observational studies. Some of the data from the following studies is shown for illustrative purposes in Fig. 1.31. [Ek and Mahrt \(1991\)](#) examined PBL relative humidity variability in a limited number of flight legs, and assumed a unimodal Gaussian fit for their distribution. Recently, [Wood and Field \(2000\)](#) studied flight data from both warm and cold clouds and reported unimodal distributions of  $q_t$ , but also observing more complex distributions, giving some weakly and strongly bimodal examples. [Davis et al. \(1996\)](#) reported uni- or bi-modal skewed distributions in liquid water content from flight data in marine stratocumulus clouds. [Larson et al. \(2001b\)](#) have also examined flight data for PBL clouds and found that mainly unimodal or bimodal distributions occurred. They reported that PDFs that included positive or negative skewness were able to give an improved fit the data. [Price \(2001\)](#) used tethered balloon data of PBL humidity collected during a three year period, finding that roughly half of the data could be classified as symmetrical or skewed unimodal. A further 25% of the data could be regarded as multimodal.

Although many of the above studies reported a significant frequency of occurrence of distributions classed as bi- or multi-modal, these distributions often possessed a single principle distribution peak, as in the example given by [Price \(2001\)](#), and thus a unimodal distribution could still offer a reasonable approximation to these cases. This also applies to the flight data examples shown in [Heymsfield and McFarquhar \(1996\)](#) taken in ice clouds. Additionally, as stated in the introduction, the bimodal and multimodal distributions may be exaggerated in both flight and balloon data. Satellite data on the other hand can give a more global view at relatively high spatial resolutions. Two such studies have been reported by [Wielicki and Parker \(1994\)](#) and ? who used Landsat data at a resolution of 28.5 meters to examine liquid water path in a large variety of cloud cover situations. They reported unimodal distributions in nearly or totally overcast scenes, and exponential-type distributions in scenes of low cloud fraction, as expected since in these cases only the tail of the  $q_t$  distribution is detected. Note that the analysis of LWP is likely to lead to much smoother (and thus more unimodal) PDFs due to the vertical integration.

In summary, it appears that in the observational data available conducted over a wide variety of cloud conditions (although rarely in ice-clouds), approximate unimodality is fairly widespread, and that a flexible unimodal function can offer a reasonable approximation to the observed variability of total water. That said, a significant minority of cases are very likely to be better modelled using a bimodal distribution like those advocated by [Lewellen and Yoh \(1993\)](#) and [Golaz et al. \(2002b\)](#).

#### 1.1.5.4 Setting the PDF moments

The second task of statistical schemes is to define the higher order moments of the distribution. If the distribution is simple, such as the uniform distribution, then it is defined by a small number of parameters. In the case of the uniform distribution, one could specify the lower or upper bounds of the distribution; two parameters are required. Equivalently, one could give the first two distribution moments: namely the mean and the variance. Likewise, more complicated PDFs that require 3 parameters can be uniquely defined using the first three moments: mean, variance and skewness;

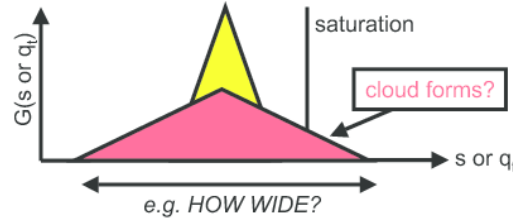


Figure 1.32: Even if the mean total water is correct, if the incorrect distribution width is diagnosed, for example the narrow yellow distribution, then clear sky conditions will prevail when in fact partial cloud cover exists (pink triangle).

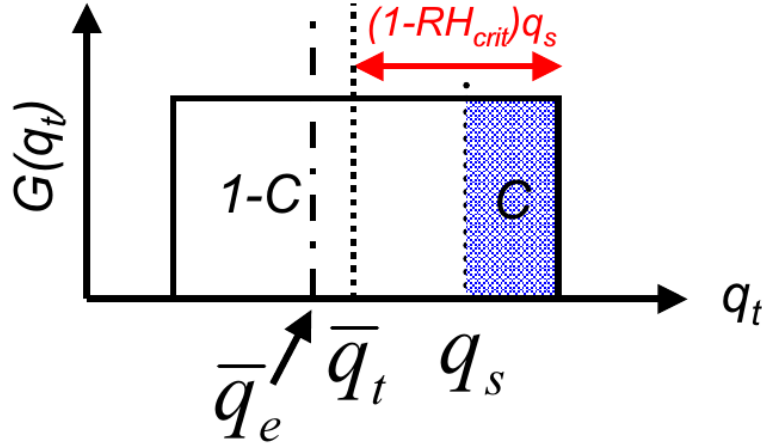


Figure 1.33: Graphical aid to the derivation of the cloud cover as a function of the  $RH$  when the total water is assumed to be uniformly distributed. If cloud begins to form at  $RH_{crit}$  then the width of the distribution is  $2q_s(1 - RH_{crit})$ . See text for details.

four-parameter distributions need the fourth moment of kurtosis (describing the PDF 'flatness', see schematic in Fig. 1.29), and so on.

It is clear to see why the accurate specification of the moments is important. The schematic of Fig. 1.32 shows that, even if the distribution mean is correct, diagnosing a variance that is too small (i.e. the distribution is too narrow) will lead to the incorrect prediction of clear sky conditions.

Some schemes diagnostically fix the higher order moments of the distribution, such as the variance. However, it is clear that this is not an ideal approach, since by having a fixed distribution width (for example), the PDF (and thus cloud properties) are not able to respond to local dynamical conditions. The fixed width (and higher order moments) are then equivalent to the specification of the critical relative humidity at which cloud is assumed to form in the  $RH$  schemes. Indeed [Smith \(1990\)](#) actually sets the width of the triangular distribution in that scheme in terms of a  $RH_{crit}$  parameter.

To illustrate fixed width schemes with a specific example, let us consider the uniform distribution adopted by [LeTreut and Li \(1991\)](#). The PDF for a typical partially cloudy grid box is shown in Fig. 1.33.

Considering the humidity, it is assumed that no supersaturation exists as is usual, and thus in the cloudy portion,  $q_v = q_s$ . Thus the grid-mean humidity can be written as:

$$\bar{q}_v = Cq_s + (1 - C)q_e \quad (1.48)$$

where  $q_e$  is the humidity in the 'environment' of the cloud; the cloud-free part of the gridbox. From the uniform distribution shape, it is possible to define  $q_e$  in terms of a critical  $RH$  for cloud formation  $RH_{crit}$ :

$$q_e = q_s(1 - (1 - C)(1 - RH_{crit})). \quad (1.49)$$

The definition of  $RH$  is  $\bar{q}_v/q_s$ , which substituting the definitions above gives

$$RH = 1 - (1 - RH_{crit})(1 - C)^2, \quad (1.50)$$

which can be rearranged to give

$$C = 1 - \sqrt{\frac{1 - RH}{1 - RH_{crit}}}. \quad (1.51)$$

This is recognised to be the relative humidity scheme used by [Sundqvist et al. \(1989\)](#)! Thus it is seen that a so-called statistical scheme with fixed moments can be reduced to a  $RH$  scheme, or likewise that  $RH$  schemes do not need to rely on ad-hoc relationships, but can be derived consistently with an assumed underlying PDF of total water. This point was fully appreciated by [Smith \(1990\)](#), whose work actually provides the  $RH$ -formulation associated with the triangular distribution in its appendix.

The example of the [Smith \(1990\)](#) scheme also raises another interesting point. Since the scheme was based on the linear  $s$  variable (see appendix below), that aims to take temperature fluctuations into account, it is often claimed that the Smith scheme (and related schemes) include the effect of temperature fluctuations. However, there is nothing in the scheme that specifically accounts for the *separate* effect of temperature fluctuations and their correlation with humidity (see [Tompkins and Giuseppe, 2003](#), for more discussion). By fixing the width of the distribution, the scheme simply defines a 'net' effect of temperature and humidity fluctuations combined. The point is that one could write the scheme purely in terms of humidity fluctuations, and arrive to the same relationship, which is witnessed by the  $RH$  derivation contained in the appendix of that paper. This in turn implies that such schemes are not, in fact, taking temperature into account in any meaningful way.

In summary, it is important to stress that there is not a clear distinction between the so-called ' $RH$  schemes' and statistical schemes. If a time-invariant variance is used in a statistical scheme, it can be reduced to a  $RH$ -type formulation and we have seen how the  $RH$  scheme of [Sundqvist et al. \(1989\)](#) can be derived by assuming a uniform distribution for total water, and likewise that the [Smith \(1990\)](#) scheme also reduces to an equivalent  $RH$  formulation.

### 1.1.6 Diagnostic versus Prognostic schemes

At this point we pause to consider the merits or otherwise of prognostic versus diagnostic cloud schemes. Shakespeare summarizes the issue well in Act III of Hamlet:

*“To be (prognostic) or not to be (prognostic), that is the question. Whether 'tis nobler in the mind to suffer, the slings and arrows of outrageous closure assumptions, or to take arms against a sea of authors, (convinced that diagnostic cloud schemes are the best), And by opposing, end them?”*

Hamlet is antagonizing over the issue of whether to implement a diagnostic or a prognostic approach in his cloud scheme. By this, we mean whether or not to include a prognostic equation for the central parameters of the scheme in question. In the case of the statistical schemes this is likely (but not necessarily) to imply a memory (a prognostic equation) for the higher order moments such as variance, where as in the Tiedtke Scheme approach outlined below the prognostic variable is the cloud cover itself.

Irrespective of the variable in question, the underlying question is always whether *the variable has a fast equilibrating timescale relative to the timestep of the model*. Let us take the case of turbulence ([Lenderink and Siebesma, 2000](#)). A highly simplified prognostic equation for variance is:

$$\frac{d\sigma^2(q_t)}{dt} = -2w'q_t \frac{dq_t}{dz} - \frac{\sigma^2(q_t)}{\tau} \quad (1.52)$$

The two terms on the RHS represent the creation of variance due to a turbulent flux of humidity occurring in the presence of a humidity gradient, and a dissipation term modelled by a Newtonian relaxation back to isotropy with a timescale of  $\tau$ . This equation is highly simplified by the neglect of both turbulent and large-scale flow transport of variance, and also the horizontal gradient terms, but it serves its illustrative purpose.

It would be possible to introduce a prognostic predictive equation for total water variance along these lines. However, if the dissipative timescale  $\tau$  is very short compared to the model timestep,

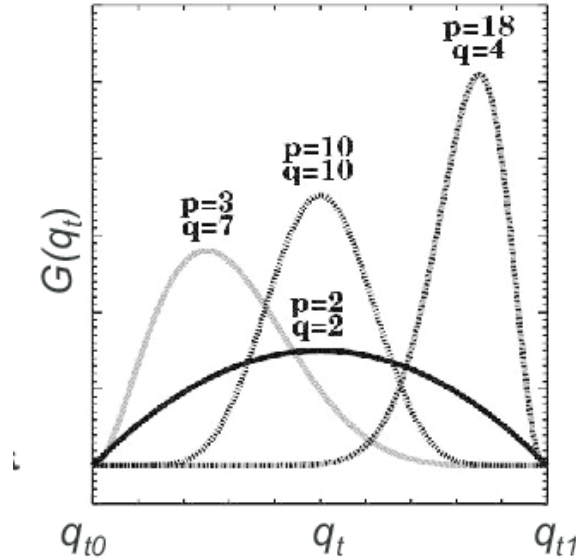


Figure 1.34: Examples of the Beta distribution for various shape parameters.

then a very good approximation could be obtained by assuming  $\frac{d\sigma^2(q_t)}{dt} = 0$ , giving

$$\sigma^2(q_t) = -2\tau \overline{w'q_t} \frac{dq_t}{dz}. \quad (1.53)$$

A diagnostic approach has the advantage that it simplifies implementation, and saves computational cost and memory. The simplification does not imply that the local cloud properties are independent of the local dynamics; a scheme based on eqn. 1.53 can not be reduced to a *RH* scheme, since the variance in each gridbox is related to the local turbulent flux. Note also that now, with such an approach, one can sensibly include the contribution of temperature fluctuations due to turbulence, as done by Ricard and Royer (1993).

For examples of this kind of approach, examine the diagnostic schemes in the literature that are described by Bougeault (1982); Ricard and Royer (1993); Bechtold et al. (1995); Lohmann et al. (1999); Chaboureau et al. (2002). These schemes mostly restrict their concern to diagnostic relationships for variance to the influence of turbulence. For example, above the boundary layer, Lohmann et al. (1999) imposed a fixed width distribution to compensate for the lack of consideration of other processes.

It is thus apparent that for generalized cloud situations, that include the evolution of clouds such as large-scale cirrus, which may evolve over many hours or even days, it will normally be necessary to resort to implementing a prognostic approach.

### 1.1.7 A prognostic statistical scheme

The first attempt to implement a fully prognostic statistical scheme into a GCM was made by Tompkins (2002). This modelled the total water fluctuations using a Beta distribution,

$$G(t) = \frac{1}{B(p, q)} \frac{(t-a)^{p-1}(b-t)^{q-1}}{(b-a)^{p+q-1}} \quad (a \leq t \leq b) \quad (1.54)$$

where  $a$  and  $b$  are the distribution limits and  $p$  and  $q$  are shape parameters (Fig. 1.34)<sup>2</sup> and the symbol  $B$  represents the Beta function, and can be defined in terms of the Gamma function,  $\Gamma$ , as follows:

$$B(p, q) = \frac{\Gamma(p)\Gamma(q)}{\Gamma(p+q)}. \quad (1.55)$$

<sup>2</sup>the original notation is repeated, but please note that the shape parameter  $q$  is not to be confused with mixing ratio,  $q_v$ .

The skewness ( $\varsigma$ ) of the distribution is related to the difference between the two shapes parameters  $p$  and  $q$ ,

$$\varsigma = \frac{2(q-p)}{p+q+2} \sqrt{\frac{p+q+1}{pq}}, \quad (1.56)$$

and thus if  $p = q$  the distribution is symmetrical, but also both positive and negatively skewed distributions are possible. As  $p$  and  $q$  tend to infinity the curve approaches the Normal distribution. The standard deviation of the distribution is given by

$$\sigma(t) = \frac{b-a}{p+q} \sqrt{\frac{pq}{p+q+1}} \quad (1.57)$$

Although this distribution is a 4-parameter function, using a simplification such as imposing  $(p-1)(q-1) = \text{constant}$  can reduce it to a three parameter distribution (Tompkins used the less satisfying  $p = \text{constant}$  closure, which unnecessarily restricted to distribution to positive skewness regimes), specified uniquely by the mean, variance and skewness of total water.

Tompkins (2002) attempted to introduce two additional prognostic equations to predict the evolution of the PDF shape. Once the distribution shape is known, (i.e. distribution limits  $a$  and  $b$  and the shape parameters  $p$  and  $q$ ) the cloud cover can be obtained from

$$C = 1 - I_{\frac{q_s-a}{b-a}}(p, q), \quad (1.58)$$

where  $I_x$  is the incomplete Beta function ratio defined as

$$I_x(p, q) = \frac{1}{B(p, q)} \int_0^x t^{p-1} (1-t)^{q-1} dt, \quad (1.59)$$

subject to the limits  $I_0(p, q) = 0$  and  $I_1(p, q) = 1$ .

Tompkins (2002) then attempted to parametrize the sources and sinks of variance and skewness separately from physical processes such as convection, turbulence, microphysics and so on. However, there is one complication that requires consideration, and is summarized by the following equation for cloud water  $q_c$ :

$$\bar{q}_c = (b-a) \frac{p}{p+q} (1 - I_{\frac{(q_s-a)}{(b-a)}}(p+1, q)) + (a-q_s) (1 - I_{\frac{(q_s-a)}{(b-a)}}(p, q)), \quad (1.60)$$

This is simply eqn. 1.47, with the Beta distribution substituted for  $G(q_t)$ . This tells us that if the distribution moments are known, then the cloud water is uniquely defined. Why is this a cause for concern? The reason is that *most cloud schemes already implement a separate prognostic equation for cloud liquid/ice water*. In other words, in partially cloudy conditions, if distribution moments *and* the cloud liquid water are given from the respective prognostic equations, then the problem is potentially over-specified. To clarify this we can re-examine the simple 2-parameter triangular distribution in Fig. 1.35. The figure shows that the 2-parameter distribution can be uniquely defined by giving either the mean and variance, or the mass mixing ratios of vapour and cloud water separately.

Thus a decision must be reached concerning the prognostic equation set to be used. The first option is to use water vapour and cloud water separately to implicitly derive the variance (right panel of Fig. 1.35). The advantage of this approach is that one does not need to explicitly derive complex variance source/sink terms, such as the impact of microphysics on variance. If, over a timestep, the microphysics reduces the cloud water (for example by autoconversion to snow, or by settling out of the gridbox) then this implicitly renders a narrowing of the distribution. Additionally it is much easier to ensure conservation of cloud water (presuming the numerics employed are designed to ensure conservation of prognostic quantities). The disadvantage is that *the information is only available in partially cloudy conditions*. In clear sky conditions one only knows the distribution mean, since  $q_c = 0$  identically (see schematic of Fig. 1.36). Likewise in overcast conditions, where  $q_v = q_s$ . In these situations, the loss of information requires supplementary ad-hoc assumptions to be made, to close the system. For example, one could resort to assuming a fixed distribution width in clear-sky conditions, thus returning to cloud formation at a specified ( $RH_{crit}$ ). We will see below that this issue arises once again in the Tiedtke (1993) scheme, which resorts to such a solution.

The second approach is to abandon the separate cloud water prognostic variable in favour of a prognostic variance equation. This has the advantage that the distribution is *always* known,

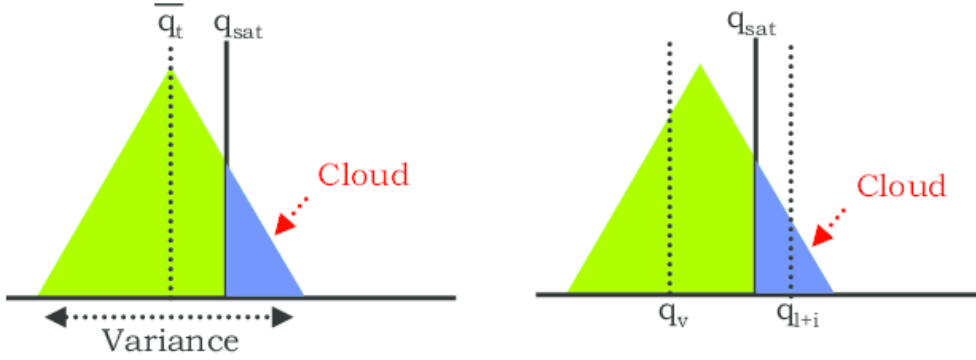


Figure 1.35: Schematic of the two ways of specifying the triangular distribution. Left Panel: The distribution mean and variance is given. Right Panel: The mean vapour and cloud water (ice+liquid) are given. In both cases the distribution is uniquely specified and the cloud cover can be diagnosed.

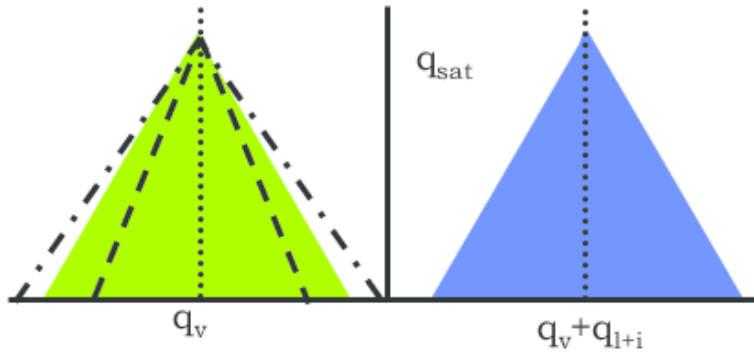


Figure 1.36: Schematic of the problem that arises if distribution width is derived from separate prognostic equations for vapour and cloud water. The curve is not uniquely defined for overcast (blue PDF) or clear sky (green PDF) conditions. For example, for the clear-sky case, there are any number of possible variances (width) of the distribution that give the correct mean water vapour and zero cloud water. Two examples are marked: a wider distribution (dot-dashed) or narrower (dotted).

even in clear sky or overcast conditions. The disadvantage is that all sources and sinks must now be parametrized in terms of variance sources and sinks. For turbulence (Deardorff, 1974), and perhaps convective sources and sinks (Lenderink and Siebesma, 2000; Klein et al., 2005), this is relatively straight-forward. However, for the microphysical processes the problem quickly becomes complicated. For simple autoconversion terms  $A$  (the rate of conversion from liquid to rain), it is possible to derive the sink of variance<sup>3</sup>

$$\frac{d\sigma^2(q_t)}{dt} = \overline{A'q_t'} = \int A'(q_t)q_t'G(q_t)dq_t, \quad (1.61)$$

which analytically tractable for simple forms of  $A$  and  $G(q_t)$ . Nevertheless, we can imagine more complicated scenarios, such as ice settling handled by a semi-Lagrangian advection scheme, allowing settling from any particular gridbox to other all levels below it. Trying to parametrize this equivalently in terms of variance sources and sinks is difficult. Moreover, by abandoning the prognostic equation for ice, any inaccuracies in the handling of such a process via a variance equa-

<sup>3</sup>Note once again the care that must be taken with regard to the numerics with long timesteps. Since autoconversion terms tend to be nonlinear they usually reduce the variance. Even if this equation is integrated implicitly for stability, the limit for long timesteps will be zero, which is unrealistic for partially cloudy conditions since the precipitation process does not affect the clear sky part of the domain. Thus instead one should integrate this term implicitly for the cloudy portion [cld] of the gridcell and then combine the result with the clear sky [clr] variance thus:  $\bar{\sigma}^2(q_t) = C(q_s^2 + \sigma^2(q_t)[cld]) + (1 - C)(q_v^2[clr] + \sigma^2(q_t)[clr]) - \bar{q}_t^2$

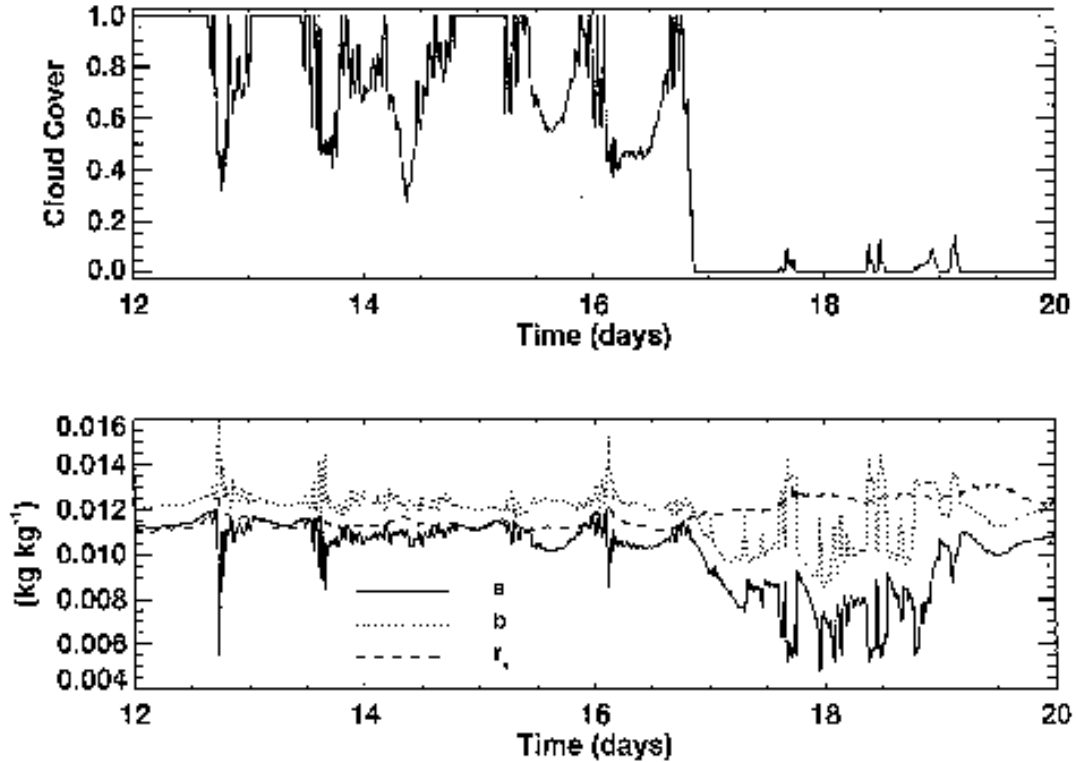


Figure 1.37: Figure taken from [Tompkins \(2002\)](#) showing evolution of the boundary layer at a gridpoint subject to stratocumulus cloud. The upper panel shows the cloud cover, while the lower panel shows the total water distribution minimum (*a*), maximum (*b*) in addition to  $q_s$  (marked  $r_s$  in the plot, according to the notation used in that paper). In the earlier period, the scene is overcast and the whole of the PDF is moister than  $q_s$ . In this case the increase in variance from turbulence breaks up the cloud deck intermittently. In the latter period instead the gridbox is relatively dry, and turbulence instead creates small cloud coverage; representing the cloud capped thermals known as 'fair weather cumulus'.

tion are likely to manifest themselves in a (potentially severe) compromising of the cloud mass conservation.

[Tompkins \(2002\)](#) tried to provide a solution for this dilemma by implementing a hybrid scheme. In partially cloudy conditions variance is derived directly from the cloud water and vapour prognostic equations. In clear sky and overcast conditions, the variance is prognosed using a subset of source and sinks terms, including turbulence, dissipation, and a highly simplified sink term due to microphysics, which is necessary in overcast conditions. The reader is referred to [Tompkins \(2002\)](#) for details of these source and sinks terms, although it should be noted that some of these, in particular the skewness budget terms from microphysics and deep convection, have been justifiably criticized by [Klein et al. \(2005\)](#) for their ad hoc nature. Nevertheless, the inclusion of even a reduced set of variance sources/sinks, especially from turbulence, is able to reproduce the observations of turbulence increasing or decreasing variance according to the mean humidity gradients, and coincidentally creating cloud or breaking-up an overcast cloud deck (Fig. 1.37).

#### 1.1.7.1 Tiedtke scheme

The ECMWF cloud cover scheme ([Tiedtke, 1993](#); [Tompkins et al., 2007](#)) is also prognostic, but rather than recording the moments of the assumed uniform total water PDF directly, it instead translates the changes in the PDF into changes in the cloud cover variable, which is integrated as the prognostic quantity. This has some advantages of simplifying some microphysical processes, but has the disadvantage that information is lost when a gridcell is either cloud-free or overcast, since in these cases  $C=1$  or  $0$  for a whole range of possible uniform distributions of total water (i.e. there is no longer a 1-1 relationship tying a unique PDF to a unique pair of values of cloud water and cloud cover). See lab exercises.

**summary** In summary, we have introduced the various approaches to diagnosing the proportion of a grid box covered by cloud in global models. The main point is that partial coverage can occur if and only if subgrid-scale fluctuations of humidity and temperature exist. All cloud schemes that predict partial cloud cover therefore implicitly or explicitly make assumptions concerning the magnitude and distribution of these fluctuations; the total water probability density function (PDF).

We discussed simple diagnostic schemes that use  $RH$  as their main or only predictor for cloud cover. We then discussed statistical schemes that explicitly specify the humidity PDF. We showed that if the moments of such schemes are time-space invariant, then the cloud cover deriving from statistical schemes can be written as diagnostic  $RH$  form. In other words, rather than using ad hoc relationships, one can derive a  $RH$ -scheme to be consistent with an underlying PDF.

It was pointed out that knowing the PDF for humidity and cloud fluctuations gives vital extra information that can be used to correct biases in nonlinear processes such as precipitation generation or interaction with radiation.

More complex statistical schemes were then discussed which attempt to predict the sources and sinks of the distribution moments, so that the PDF can realistically respond to the various relevant atmospheric processes. The lecture dwelled on the choice of the prognostic variables, in particular whether it is preferable to predict the PDF moments themselves, or instead to predict integrated and direct cloud quantities such as the cloud liquid water. Advantages and potential drawbacks of each approach were discussed; which were essentially that by directly predicting the cloud variables, one ensures their conservation, and processes such as microphysics are far easier to handle, but that in clear sky or overcast conditions there is lack of information so that diagnostic/fixed assumptions have to be made concerning the subgrid distribution in these situations. These assumptions may also lead to a lack of “reversibility” in this approach.

It was pointed out that the Tiedtke scheme is essentially a manifestation of the second approach, where both cloud water *and* cloud cover are predicted, and where often an underlying assumption concerning the humidity and cloud distribution is made to derive the sources and sinks of these prognostic variables. We highlighted that, while proven successful in NWP, the scheme suffers from the same drawback of requiring the implementation of a fixed (independent of local dynamical conditions)  $RH_{crit}$  for cloud formation and a lack of reversibility.

### 1.1.8 Cloud overlap

Cloud schemes must also consider how cloud overlap in the vertical.

Some common assumptions includes the

- Maximum
- Random
- Maximum-Random (Random if clouds separately by a clear layer)
- Exponential-random (Maximum overlap in vertically contiguous clouds decays exponentially with distance)

some of these assumptions are shown in Fig. 1.38.

The maximum overlap assumption assumes that the clouds are maximally correlated in the vertical, thus minimizing cloud overlap. Thus the overall cloud cover  $C_{i,j}$  of layers  $i$  and  $j$  is simply:

$$C_{i,j}^{max} = \max(C_i, C_j) \quad (1.62)$$

Random overlap instead assumes that cloudy layers are randomly distributed.

$$C_{i,j}^{ran} = C_i + C_j - C_i C_j \quad (1.63)$$

An infrequently used assumption of minimum overlap assumes that mutually exclusivity leads to a maximal cloud coverage.

The combined max-ran scheme is still widely used in models, and assumes that adjacent cloudy layers are maximally overlapped, while layers separated by a clear layer are randomly overlapped.

A final recently developed scheme is known as the EXP-RAN scheme Hogan and Illingworth (2000), which is a generalization of the MAX-RAN scheme (Fig/ 1.39).

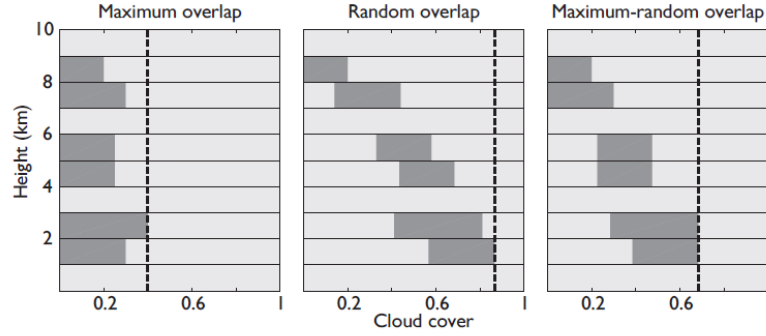


Figure 1.38: Schematic of the macroscale parametrization problem

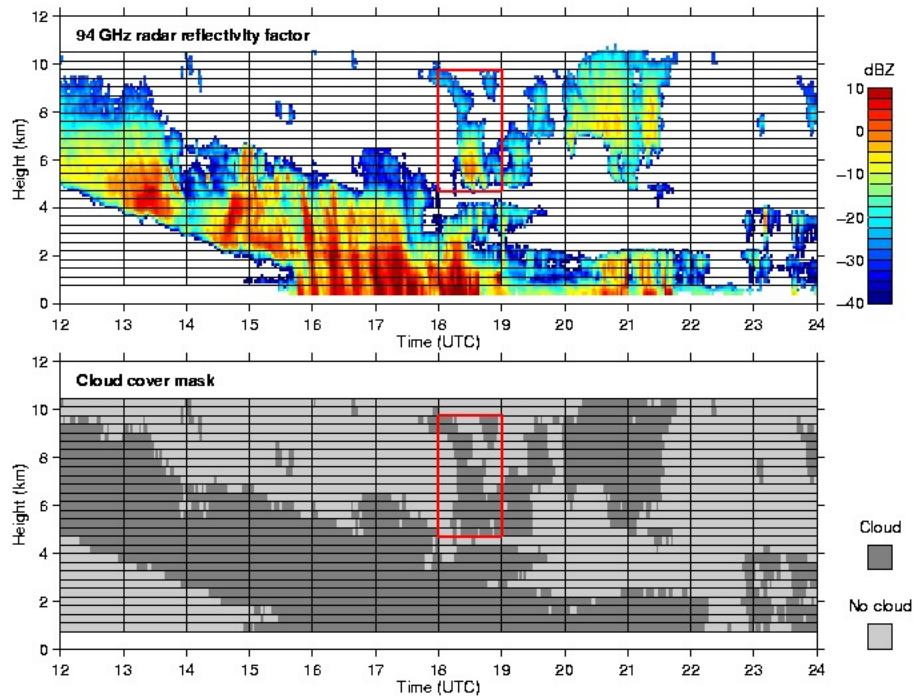


Figure 1.39: schematic of cloud overlap from Reading University and Hogan and Illingworth (2000)

It still assumes that the overlap in continually cloudy adjacent layers, decorrelates according to a scale height  $\tau$ , while layers separated by a clear layer are still randomly overlapped. Thus for continually cloudy layers:

$$C_{i,j}^{exp-ran} = \alpha C_{i,j}^{max} + (1 - \alpha) C_{i,j}^{ran} \quad (1.64)$$

where  $\alpha$  has been parameterized as

$$\alpha = \exp\left(-\frac{D}{\tau}\right) \quad (1.65)$$

where various values have been derived for  $\tau$ , with Hogan and Illingworth (2000) giving a value of 2 km. Further generalizations of this scheme incorporate solar geometry Tompkins and Giuseppe (2007) and wind shear Giuseppe and Tompkins (2015).

It is clear that combining overlap, subgrid partial cloud cover, sub-cloud variability, the situation can get complicated (Fig. 1.40)! It is clear that there will always be a need for diagnostic closure assumptions concerning sub-grid scale geometrical and microphysical effects, no matter how much resolution one throws at a problem!

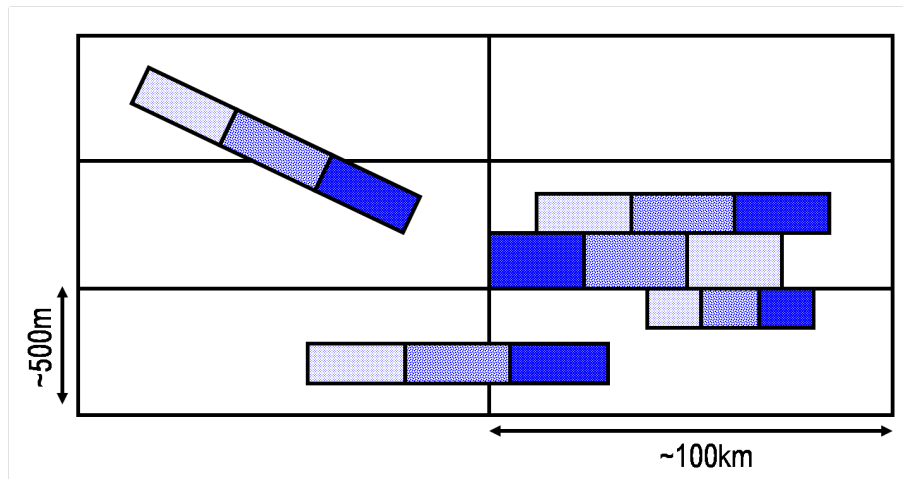


Figure 1.40: Schematic of the macroscale parametrization problem

Take home messages

- **Resolution** determines the finest scale of motions that can be explicitly modelled; the truncation scale. The effect on the grid-resolved scale of any process occurring on smaller spatial scales than this has to be **parameterized**.
- **Parameterizations** are models for small scale processes *written in terms of grid-scale variables*. The way this is done can be guided by observations, higher resolution models or theory, but they can never be exact, since the small scales are not explicitly modelled. Essentially an attempt is made to model the statistics of the phenomena.
- Computing resources need to be shared between **model resolution, timestep (=accuracy), complexity of physics parametrization and number of ensemble members**

# Bibliography

- Arakawa, A., and W. H. Shubert, 1974: Interaction of a cumulus ensemble with the large-scale environment. Part 1. *J. Atmos. Sci.*, **31**, 674–701.
- Barker, H. W., G. L. Stephens, and Q. Fu, 1999: The sensitivity of domain-averaged solar fluxes to assumptions about cloud geometry. *Q. J. R. Meteorol. Soc.*, **125**, 2127–2152.
- Barker, H. W., B. A. Wielicki, and L. Parker, 1996: A parameterization for computing grid-averaged solar fluxes for inhomogeneous marine boundary layer clouds. Part II: Validation using satellite data. *J. Atmos. Sci.*, **53**, 2304–2316.
- Bechtold, P., J. W. M. Cuijpers, P. Mascart, and P. Trouilhet, 1995: Modeling of trade-wind cumuli with a low-order turbulence model - toward a unified description of Cu and Sc clouds in meteorological models. *J. Atmos. Sci.*, **52**, 455–463.
- Bechtold, P., C. Fravallo, and J. P. Pinty, 1992: A model of marine boundary-layer cloudiness for mesoscale applications. *J. Atmos. Sci.*, **49**, 1723–1744.
- Beheng, K. D., 1994: A parameterization of warm rain cloud microphysical processes. *Atmos. Res.*, **33**, 193–206.
- betts, A. K., 1986: A new convective adjustment scheme. part 1: Observation and theoretical basis. *Q. J. R. Meteorol. Soc.*, **112**, 677–691.
- Betts, A. K., and M. J. Miller, 1986: A new convective adjustment scheme. Part 2: Single column tests using GATE WAVE, BOMEX, ATEX and arctic air-mass data sets. *Q. J. R. Meteorol. Soc.*, **112**, 693–709.
- Bony, S., and K. A. Emanuel, 2001: A parameterization of the cloudiness associated with cumulus convection: Evaluation using TOGA COARE data. *J. Atmos. Sci.*, **58**, 3158–3183.
- Bougeault, P., 1982: Cloud ensemble relations based on the Gamma probability distribution for the high-order models of the planetary boundary layer. *J. Appl. Meteor.*, **39**, 2691–2700.
- Cahalan, R. F., W. Ridgway, W. J. Wiscombe, T. L. Bell, and J. B. Snider, 1994: The albedo of fractal stratocumulus clouds. *J. Atmos. Sci.*, **51**, 2434–2455.
- Chaboureaud, J. P., J. P. Cammas, P. J. Mascart, J. P. Pinty, and J. P. Lafore, 2002: Mesoscale model cloud scheme assessment using satellite observations. *J. Geophys. Res.*, **107**, doi: 10.1029/2001JD000714.
- Cusack, S., J. M. Edwards, and R. Kershaw, 1999: Estimating the subgrid variance of saturation, and its parametrization for use in a GCM cloud scheme. *Q. J. R. Meteorol. Soc.*, **125**, 3057–3076.
- Davis, A., A. Marshak, W. Wiscombe, and R. Cahalan, 1996: Scale invariance of liquid water distributions in marine stratocumulus. Part I: Spectral properties and stationarity issues. *J. Atmos. Sci.*, **53**, 1538–1558.
- de Roode, S. R., P. G. Duynkerke, and A. P. Siebesma, 2000: Analogies between mass-flux and Reynolds-averaged equations. *J. Atmos. Sci.*, **57** (10), 1585–1598.
- Deardorff, J. W., 1974: Three dimensional numerical study of turbulence in an entraining mixed layer. *Bound.-Layer Meteor.*, **7**, 199–226.

- Dessler, A. E., and P. Yang, 2003: The distribution of tropical thin cirrus clouds inferred from terra MODIS data. *J. Climate*, **16**, 1241–1247.
- Ek, M., and L. Mahrt, 1991: A formulation for boundary-layer cloud cover. *Ann. Geophysicae*, **9**, 716–724.
- Emanuel, K. A., 1991: A scheme for representing cumulus convection in large-scale models. *J. Atmos. Sci.*, **48**, 2313–2335.
- Fowler, L. D., D. A. Randall, and S. A. Rutledge, 1996: Liquid and ice cloud microphysics in the CSU general circulation model. Part I: Model description and simulated cloud microphysical processes. *J. Climate*, **9**, 489–529.
- Fu, Q., B. Carlin, and G. Mace, 2000: Cirrus horizontal inhomogeneity and OLR bias. *Geophys. Res. Lett.*, **27**, 3341–3344.
- Gierens, K., U. Schumann, M. Helten, H. Smit, and P. H. Wang, 2000: Ice-supersaturated regions and subvisible cirrus in the northern midlatitude upper troposphere. *J. Geophys. Res.*, **105**, 22 743–22 753.
- Giuseppe, F. D., and A. M. Tompkins, 2003: Three dimensional radiative transfer in tropical deep convective clouds. *J. Geophys. Res.*, **108**, 10.1029/2003JD003 392.
- Giuseppe, F. D., and A. M. Tompkins, 2015: Generalizing cloud overlap treatment to include the effect of wind shear. *J. Atmos. Sci.*, **72**, 2865–2876.
- Golaz, J., V. E. Larson, and W. R. Cotton, 2002a: A PDF-based parameterization for boundary layer clouds. Part I: Method and model description. *J. Atmos. Sci.*, **59**, 3540–3551.
- Golaz, J., V. E. Larson, and W. R. Cotton, 2002b: A PDF-based parameterization for boundary layer clouds. Part II: Model results. *J. Atmos. Sci.*, **59**, 3552–3571.
- Heymsfield, A. J., and G. M. McFarquhar, 1996: High albedos of cirrus in the Tropical Pacific Warm Pool: Microphysical interpretations from CEPEX and from Kwajalein, Marshall Islands. *J. Atmos. Sci.*, **53**, 2424–2451.
- Heymsfield, A. J., L. M. Miloshevich, C. Twohy, G. Sachse, and S. Oltmans, 1998: Upper-tropospheric relative humidity observations and implications for cirrus ice nucleation. *Geophys. Res. Lett.*, **25**, 1343–1346.
- Hogan, R. J., and A. J. Illingworth, 2000: Deriving cloud overlap statistics from radar. *Q. J. R. Meteorol. Soc.*, **126**, 2903–2909.
- Jakob, C., 2003: An Improved Strategy for the Evaluation of Cloud Parameterizations in GCMs. *Bull. Amer. Meteor. Soc.*, **84**, 1387–1401.
- Kessler, E., 1969: *On the Distribution and Continuity of Water Substance in Atmospheric Circulation*, *Meteorological Monography*, 10. American Meteorological Society.
- Kitchen, M., R. Brown, and A. G. Davies, 1994: Real-time correction of weather radar data for the effects of bright band, range and orographic growth in widespread precipitation. *Q. J. R. Meteorol. Soc.*, **120**, 1231–1254.
- Klein, S. A., R. Pincus, C. Hannay, and K.-M. Xu, 2005: Coupling a statistical scheme to a mass flux scheme. *J. Geophys. Res.*, **110**, 10.1029/2004JD005 017.
- Krüger, S. K., 1988: Numerical simulation of tropical cumulus clouds and their interaction with the subcloud layer. *J. Atmos. Sci.*, **45** (16), 2221–2250.
- Larson, V. E., R. Wood, P. R. Field, J. Golaz, T. H. VonderHaar, and W. R. Cotton, 2001a: Small-scale and mesoscale variability of scalars in cloudy boundary layers: One dimensional probability density functions. *J. Atmos. Sci.*, **58**, 1978–1994.
- Larson, V. E., R. Wood, P. R. Field, J.-C. Golaz, T. H. VonderHaar, and W. R. Cotton, 2001b: Systematic biases in the microphysics and thermodynamics of numerical models that ignore subgrid-scale variability. *J. Atmos. Sci.*, **58**, 1117–1128.

- Lenderink, G., and A. P. Siebesma, 2000: Combining the massflux approach with a statistical cloud scheme. *Proc. 14th Symp. on Boundary Layers and Turbulence*, Amer. Meteor. Soc., Aspen, CO, USA, 66–69.
- LeTreut, H., and Z. X. Li, 1991: Sensitivity of an atmospheric general circulation model to prescribed SST changes: Feedback effects associated with the simulation of cloud optical properties. *Climate Dynamics*, **5**, 175–187.
- Lewellen, W. S., and S. Yoh, 1993: Binormal model of ensemble partial cloudiness. *J. Atmos. Sci.*, **50**, 1228–1237.
- Liu, Y., P. H. Daum, R. McGraw, and R. Wood, 2006: Parameterization of the autoconversion process. PART II: Generalization of Sundqvist-type parameterizations. *J. Atmos. Sci.*, **63** (3), 1103–1109.
- Lohmann, U., N. McFarlane, L. Levkov, K. Abdella, and F. Albers, 1999: Comparing different cloud schemes of a single column model by using mesoscale forcing and nudging technique. *J. Climate*, **12**, 438–461.
- Lohmann, U., and E. Roeckner, 1996: Design and performance of a new cloud microphysics scheme developed for the ECHAM general circulation model. *Climate Dynamics*, **12**, 557–572.
- Manabe, S., and R. F. Strickler, 1964: Thermal equilibrium of the atmosphere with a convective adjustment. *J. Atmos. Sci.*, **21**, 361–385.
- Mellor, G. L., 1977: Gaussian cloud model relations. *J. Atmos. Sci.*, **34**, 356–358.
- Nishizawa, K., 2000: Parameterization of nonconvective condensation for low-resolution climate models: Comparison of diagnostic schemes for fractional cloud cover and cloud water content. *J. Meteor. Soc. Japan*, **78**, 1–12.
- Ose, T., 1993: An examination of the effects of explicit cloud water in the UCLA GCM. *J. Meteor. Soc. of Japan*, **71**, 93–109.
- Paluch, I. R., 1979: The Entrainment Mechanism in Colorado Cumuli. *J. Atmos. Sci.*, **36**, 2467–2478.
- Pincus, R., and S. A. Klein, 2000: Unresolved spatial variability and microphysical process rates in large-scale models. *J. Geophys. Res.*, **105**, 27 059–27 065.
- Pomroy, H. R., and A. J. Illingworth, 2000: Ice cloud inhomogeneity: Quantifying bias in emissivity from radar observations. *Geophys. Res. Lett.*, **27**, 2101–2104.
- Price, J. D., 2001: A study on boundary layer humidity distributions and errors in parameterised cloud fraction. *Q. J. R. Meteorol. Soc.*, **127**, 739–759.
- Randall, D. A., M. Khairoutdinov, A. Arakawa, and W. Grabowski, 2003: Breaking the cloud parameterization deadlock. *Bull. Amer. Meteor. Soc.*, **84**, 1547–1564.
- Raymond, D. J., and A. M. Blyth, 1986: A stochastic mixing model for nonprecipitating cumulus clouds. *J. Atmos. Sci.*, **43**, 2708–2718.
- Ricard, J. L., and J. F. Royer, 1993: A statistical cloud scheme for use in an AGCM. *Ann. Geophysicae*, **11**, 1095–1115.
- Roeckner, E., and Coauthors, 1996: The atmospheric general circulation model ECHAM4: Model description and simulation of present-day climate. Tech. rep., Max Planck Institute for Meteorology, Bundesstrasse 55, 20146 Hamburg, Germany.
- Rotstayn, L. D., 1997: A physically based scheme for the treatment of stratiform precipitation in large-scale models. I: Description and evaluation of the microphysical processes. *Q. J. R. Meteorol. Soc.*, **123**, 1227–1282.
- Rotstayn, L. D., 2000: On the "tuning" of autoconversion parameterizations in climate models. *J. Geophys. Res.*, **105**, 15 495–15 507.

- Simpson, J., and V. Wiggert, 1969: Models of precipitating cumulus towers. *Mon. Wea. Rev.*, **97**, 471–489.
- Slingo, J. M., 1980: A cloud parametrization scheme derived from GATE data for use with a numerical-model. *Q. J. R. Meteorol. Soc.*, **106**, 747–770.
- Slingo, J. M., 1987: The development and verification of a cloud prediction scheme for the ECMWF model. *Q. J. R. Meteorol. Soc.*, **113**, 899–927.
- Smith, R. N. B., 1990: A scheme for predicting layer clouds and their water-content in a general-circulation model. *Q. J. R. Meteorol. Soc.*, **116**, 435–460.
- Sommeria, G., and J. W. Deardorff, 1977: Subgrid-scale condensation in models of nonprecipitating clouds. *J. Atmos. Sci.*, **34**, 344–355.
- Spichtinger, P., K. Gierens, and W. Read, 2003: The global distribution of ice-supersaturated regions as seen by the Microwave Limb Sounder. *Q. J. R. Meteorol. Soc.*, **129**, 3391–3410.
- Sundqvist, H., E. Berge, and J. E. Kristjansson, 1989: Condensation and cloud parameterization studies with a mesoscale numerical weather prediction model. *Mon. Wea. Rev.*, **117**, 1641–1657.
- Tiedtke, M., 1989: A comprehensive mass flux scheme for cumulus parameterization in large-scale models. *Mon. Wea. Rev.*, **117**, 1779–1800.
- Tiedtke, M., 1993: Representation of clouds in large-scale models. *Mon. Wea. Rev.*, **121**, 3040–3061.
- Tompkins, A. M., 2002: A prognostic parameterization for the subgrid-scale variability of water vapor and clouds in large-scale models and its use to diagnose cloud cover. *J. Atmos. Sci.*, **59**, 1917–1942.
- Tompkins, A. M., and K. A. Emanuel, 2000: The vertical resolution sensitivity of simulated equilibrium temperature and water vapour profiles. *Q. J. R. Meteorol. Soc.*, **126**, 1219–1238.
- Tompkins, A. M., K. Gierens, and G. Rädcl, 2007: Ice supersaturation in the ECMWF integrated forecast system. *Q. J. R. Meteorol. Soc.*, **133**, 53–63.
- Tompkins, A. M., and F. D. Giuseppe, 2003: Solar radiative biases in deep convective regimes: Possible implications for dynamical feedback. *Q. J. R. Meteorol. Soc.*, **129**, 1721–1730.
- Tompkins, A. M., and F. D. Giuseppe, 2007: Generalizing cloud overlap treatment to include solar zenith angle effects on cloud geometry. *J. Atmos. Sci.*, **64**, 2116–2125.
- Wielicki, B. A., and L. Parker, 1994: Frequency distributions of cloud liquid water path in oceanic boundary layer cloud as a function of regional cloud fraction. *Proc. Eighth Conference on Atmospheric Radiation*, Amer. Meteor. Soc., Nashville, TN, USA, 415–417.
- Wood, R., and P. R. Field, 2000: Relationships between total water, condensed water, and cloud fraction in stratiform clouds examined using aircraft data. *J. Atmos. Sci.*, **57**, 1888–1905.
- Xu, K.-M., and D. A. Randall, 1996: A semiempirical cloudiness parameterization for use in climate models. *J. Atmos. Sci.*, **53**, 3084–3102.
- Yanai, M., S. Esbensen, and J.-H. Chu, 1973: Determination of bulk properties of tropical cloud clusters from large-scale heat and moisture budgets. *J. Atmos. Sci.*, **30** (4), 611–627.